Biogeosciences Discuss., 11, 17043–17087, 2014
www.biogeosciences-discuss.net/11/17043/2014/
doi:10.5194/bgd-11-17043-2014

Biogeosciences
Discussions
Open Access

Export fluxes in a naturally fertilized area of the Southern Ocean, the Kerguelen Plateau: seasonal dynamic reveals long lags and strong attenuation of particulate organic carbon flux (Part 1)

M. Rembauville[1,2], I. Salter[1,2,3], N. Leblond[4,5], A. Gueneugues[1,2], and S. Blain[1,2]

[1]Sorbonne Universités, UPMC Univ Paris 06, UMR 7621, LOMIC, Observatoire Océanologique, Banyuls-sur-Mer, France
[2]CNRS, UMR 7621, LOMIC, Observatoire Océanologique, Banyuls-sur-Mer, France
[3]Alfred-Wegener-Institute for Polar and Marine research, Bremerhaven, Germany
[4]Sorbonne Universités, UPMC Univ Paris 06, LOV, UMR 7093, Observatoire Océanologique, Villefranche-sur-Mer, France
[5]CNRS-INSU, LOV, UMR 7093, Observatoire Océanologique, Villefranche-sur-Mer, France

Received: 7 November 2014 – Accepted: 13 November 2014 – Published: 10 December 2014

Correspondence to: M. Rembauville (rembauville@obs-banyuls.fr)

Published by Copernicus Publications on behalf of the European Geosciences Union.

Abstract

A sediment trap moored in the naturally iron-fertilized Kerguelen plateau in the Southern Ocean provided an annual record of particulate organic carbon and nitrogen fluxes at 289 m. At the trap deployment depth current speeds were low ($\sim 10\,\mathrm{cm\,s^{-1}}$) and primarily tidal-driven (M2 tidal component) providing favorable hydrodynamic conditions for the collection of flux. Particulate organic carbon (POC) flux was generally low ($< 0.5\,\mathrm{mmol\,m^{-2}\,d^{-1}}$) although two episodic export events (< 14 days) of $1.5\,\mathrm{mmol\,m^{-2}\,d^{-1}}$ were recorded. These increases in flux occurred with a 1 month time lag from peaks in surface chlorophyll and together accounted for approximately 40 % of the annual flux budget. The annual POC flux of $98.2 \pm 4.4\,\mathrm{mmol\,m^{-2}\,yr^{-1}}$ was relatively low considering the shallow deployment depth, but similar to deep-ocean (> 2 km) fluxes measured from similarly productive iron-fertilized blooms. Comparison of the sediment trap data with complementary estimates of biomass accumulation and export indicate that ~ 90 % of the flux was lost between 200 and 300 m. We hypothesize that grazing pressure, including mesozooplankton and mesopelagic fishes, may be responsible for rapid flux attenuation and the High Biomass Low Export regime characterizing the Kerguelen bloom. The importance of plankton community structure in controlling the temporal variability of export fluxes is addressed in a companion paper.

1 Introduction

The biological carbon pump is defined as the vertical transfer of biologically fixed carbon in the ocean surface to the ocean interior (Volk and Hoffert, 1985). Global estimates of Particulate Organic Carbon (POC) export cluster between $5\,\mathrm{Pg\,C\,yr^{-1}}$ (Moore et al., 2004; Lutz et al., 2007; Honjo et al., 2008; Henson et al., 2011; Lima et al., 2014a) to $10\,\mathrm{Pg\,C\,yr^{-1}}$ (Laws et al., 2000; Schlitzer, 2004; Gehlen et al., 2006; Boyd and Trull, 2007; Dunne et al., 2007; Laws et al., 2011). Nevertheless, the physical transfer of dissolved inorganic carbon to the ocean interior during subduction of water masses is two orders of magnitude higher ($> 250\,\mathrm{Pg\,C\,yr^{-1}}$, Karleskind et al., 2011; Levy et al., 2013). The global ocean represents a net annual CO_2 sink of $2.5\,\mathrm{Pg\,C\,yr^{-1}}$ (Le Quéré et al., 2013), slowing down the increase of the atmospheric CO_2 concentration resulting from anthropogenic activity. Although the Southern Ocean (south of 44° S) plays a limited role in the net air–sea CO_2 flux (Lenton et al., 2013), it is a key component of the global anthropogenic CO_2 sink representing one third the global oceanic sink ($\sim 1\,\mathrm{Pg\,C\,yr^{-1}}$) while covering 20 % of its surface (Gruber et al., 2009). The solubility pump is considered as the major component of this sink.

Following it's hypothesis in the nineties (Martin, 1990), iron limitation of high nutrient low chlorophyll (HNLC) areas, including the Southern Ocean, has been tested in bottle experiments (de Baar et al., 1990) and through in situ artificial fertilization experiments (de Baar et al., 2005; Boyd et al., 2007). Results from these experiments are numerous and essentially highlight that iron limits macronutrient (N, P, Si) utilization (Boyd et al., 2005; Hiscock and Millero, 2005) and primary production (Landry et al., 2000; Gall et al., 2001; Coale et al., 2004) in these vast HNLC areas of the Southern Ocean. Due to a large macronutrient repository the biological carbon pump in the Southern Ocean is considered to be inefficient in its capacity to transfer atmospheric carbon to the ocean interior (Sarmiento and Gruber, 2006). In the context of micronutrient limitation, sites enriched in iron by natural processes have also been studied and include the Kerguelen islands (Blain et al., 2001, 2007), the Crozet islands (Pollard et al., 2007), the Scotia Sea (Tarling et al., 2012), and the Drake Passage (Measures et al., 2013). Enhanced primary producer biomass in association with natural iron supply (Korb and Whitehouse, 2004; Seeyave et al., 2007; Lefèvre et al., 2008) strongly support trace-metal limitation. Furthermore, indirect seasonal budgets constructed from studies of naturally fertilized systems have been capable of demonstrating an increase in the strength of the biological carbon pump (Blain et al., 2007; Pollard et al., 2009), although strong discrepancies in carbon to iron sequestration efficiency exist between systems. To date, direct measurements of POC export from naturally fertilized blooms in the Southern Ocean are limited to the Crozet Plateau (Pollard et al., 2009; Salter et al., 2012). The HNLC Southern Ocean represents a region where changes in the strength of the biological pump may have played a role in the glacial–interglacial CO_2 cycles (Bopp et al., 2003; Kohfeld et al., 2005) and have some significance to future anthropogenic CO_2 uptake (Sarmiento and Le Quéré, 1996). In this context, additional studies that directly measure POC export from naturally iron-fertilized blooms in the Southern Ocean are necessary.

POC export can be estimated at short timescales (days to weeks) using the ^{234}Th proxy (Coale and Bruland, 1985; Buesseler et al., 2006; Savoye et al., 2006), by optical imaging of particles (e.g. Picheral et al., 2010) or by directly collecting particles into surface-tethered sediment traps (e.g. Maiti et al., 2013 for a compilation in the Southern Ocean) or neutrally buoyant sediment traps (e.g. Salter et al., 2007; Rynearson et al., 2013). Temporal variability of flux in the Southern Ocean precludes extrapolation of discrete measurements to estimate seasonal or annual carbon export. However seasonal export of POC can be derived from biogeochemical budgets (Blain et al., 2007; Pollard et al., 2009) or be directly measured by moored sediment traps (e.g. Salter et al., 2012). Biogeochemical budgets are capable of integrating over large spatial and temporal scales but may incorporate certain assumptions and lack information about underlying mechanisms. Direct measurement by sediment traps rely on fewer assumptions but their performance is strongly related to prevailing hydrodynamic conditions (Buesseler et al., 2007a), which can be particularly problematic in the surface ocean. Measuring the hydrological conditions characterizing mooring deployments is necessary to address issues surrounding the efficiency of sediment trap collection.

The ecological processes responsible for carbon export remain poorly characterized (Boyd and Trull, 2007). Having direct access to the exported material in a quantitative way can elucidate patterns in carbon and biomineral fluxes to the ocean interior (Francois et al., 2002; Henson et al., 2012; Le Moigne et al., 2012; Lima et al., 2014). Long-term deployment of moored sediment traps in areas of naturally iron fertilized production, where significant macro- and micro-nutrient gradients seasonally structure plankton communities, can help to establish links between ecological succession and carbon export. For example, sediment traps around the Crozet Plateau (Pollard et al., 2009) identified the significance of *Eucampia antarctica var. antarctica* resting spores for carbon transfer to the deep ocean, large empty diatom frustules for Si:C export stoichiometry (Salter et al., 2012), and heterotrophic calcifiers for the carbonate counter pump (Salter et al., 2014).

The increase in primary production resulting from natural fertilization might not necessarily lead to significant increases in carbon export. The concept of “High Biomass, Low Export” (HBLE) environments was first introduced in the Southern Ocean (Lam and Bishop, 2007). This concept is partly based on the idea that a strong grazer response to phytoplankton biomass leads to major fragmentation and remineralization of particles in the twilight zone, shallowing the remineralization horizon (Coale et al., 2004). Alternative explanations suggest that the efficient utilization and reprocessing of exported carbon by zooplankton leads to fecal pellet dominated, low POC fluxes (Ebersbach et al., 2011). A synthesis of short-term sediment trap deployments, ^{234}Th estimates of upper ocean POC export and in situ primary production measurements in the Southern Ocean by Maiti et al. (2013) has highlighted the inverse relationship between primary production and export efficiency, verifying the HBLE status of many productive areas in the Southern Ocean. The iron fertilized bloom above the Kerguelen Plateau exhibits strong remineralization in the mixed layer compared to the mesopelagic (Jacquet et al., 2008) and high bacterial carbon demand (Obernosterer et al., 2008), features consistent with a HBLE regime. Moreover, an inverse relationship between export efficiency and zooplankton biomass in the Kerguelen Plateau region support the key role of grazers in the HBLE scenario (Laurenceau et al., 2014a). Efficient grazer responses to phytoplankton biomass following artificial iron fertilization of HNLC regions also demonstrate increases in net community production that are not translated to an increase in export fluxes (Lam and Bishop, 2007; Martin et al., 2013; Batten and Gower, 2014).

POC flux attenuation with depth results from processes occurring in the euphotic layer (setting the particle export efficiency, Henson et al., 2012) and processes occurring in the twilight zone between the euphotic layer and ~ 1000 m (Buesseler and Boyd, 2009), setting the transfer efficiency (Francois et al., 2002). These processes are mainly biologically-driven (Boyd and Trull, 2007) and involve a large diversity of ecosystem components from bacteria (Rivkin and Legendre, 2001; Giering et al., 2014), protozooplankton (Barbeau et al., 1996), mesozooplankton (Dilling and Alldredge, 2000; Smetacek et al., 2004) and mesopelagic fishes (Davison et al., 2013; Hudson et al., 2014). The net effect these processes is summarized in a power-law formulation of POC flux attenuation with depth proposed by Martin et al. (1987) that is still commonly used in data and model applications. The b-exponent in this formulation has been reported to range from 0.4 to 1.7 (Buesseler et al., 2007b; Lampitt et al., 2008; Henson et al., 2012) in the global Ocean. Nevertheless, a change in the upper mesopelagic community structure (Lam et al., 2011), and more precisely an increasing contribution of mesozooplankton (Lam and Bishop, 2007; Ebersbach et al., 2011) could lead to a shift toward higher POC flux attenuation with depth.

The aims of this paper are (1) to provide the first annual description of the POC and PON export fluxes below the mixed layer within the naturally fertilized bloom of the Kerguelen Plateau, (2) to discuss the reliability of these measurements considering the hydrological and biological context, (3) to compare the results with other estimates of POC fluxes made on different time-scales from KEOPS1 and KEOPS2 and (4) to suggest hypothesis explaining the flux attenuation. A companion paper (Rembauville et al., 2014) addresses our final aim: to identify the ecological vectors that explain the intensity and the stoichiometry of the fluxes.

2 Material and methods

2.1 Trap deployment and mooring design

As part of the KEOPS2 multidisciplinary program, a mooring line was deployed at station A3 (50°38.3′ S–72°02.6′ E) in the Permanently Open Ocean Zone (POOZ), south of the Polar Front (PF) (Fig. 1). The mooring line was instrumented with a Technicap PPS3 (0.125 m^2 collecting area, 4.75 aspect ratio) sediment trap and inclinometer (NKE S2IP) at a depth of 289 m (seafloor depth 527 m) (Fig. 2). A conductivity-temperature-pressure (CTD) sensor (Seabird SBE 37) and a current meter (Nortek Aquadopp) were placed on the mooring line 30 m beneath the sediment trap (319 m). The sediment trap collection period started on 21 October 2011 until 7 September 2012. The sediment trap was composed of twelve rotating sample cups (250 mL) filled with a 5 % formalin hypersaline solution buffered with sodium tetraborate at pH = 8. Rotation of the carousel was programmed to sample short intervals (10–14 days) between October and February, to optimize the temporal resolution of export from the bloom, and long intervals (99 days) between February and September. All instruments had a 1 h recording interval. The current meter failed on the 7 April 2012.

2.2 Surface chlorophyll data

The MODIS AQUA level 3 (4 km grid resolution, 8 day averages) surface chlorophyll *a* product was extracted from the NASA website (http://oceancolor.gsfc.nasa.gov/) for sediment trap deployment period. An annual climatology of surface chlorophyll *a* concentration, based on available satellite products (1997–2013), was calculated from the multisatellite Globcolour product. The Globcolour level 3, (case 1 waters, 4.63 km resolution, 8 day averages) product merging Seawifs, MODIS and MERIS data with GSM merging model (Maritorena and Siegel, 2005) was accessed via http://www.globcolour.info. Surface chlorophyll *a* concentrations derived from Globcolour (climatology) and MODIS data (deployment year) were averaged across a 100 km radius centered on the sediment trap deployment location (Fig. 1).

2.3 Time series analyses of hydrological parameters

Fast Fourier Transform (FFT) analysis was performed on the annual time series data obtained from the mooring, depth and potential density anomalies (σ_θ) that were derived from the CTD sensor. Significant peaks in the power spectrum were identified by comparison to red noise, a theoretical signal in which the relative variance decreases with increasing frequency (Gilman et al., 1963). The red noise signal was considered as a null hypothesis and its power spectrum was scaled to the 99th percentile of χ^2 probability. Power peaks higher than 99 % red noise values were considered to be statistically significant (Schulz and Mudelsee, 2002), enabling the identification of periods of major variability in time series. In order to identify the water masses surrounding the trap, temperature and salinity recorded by the mooring CTD were placed in context to previous CTD casts conducted at A3 during KEOPS1 (39 profiles, 23 January 2005–13 February 2005) and KEOPS2 (12 profiles, from 15–17 November).

2.4 Sediment trap material analyses

Upon recovery of the sediment trap the pH of the supernatant was measured and 1 mL of 37 % formalin buffered with sodium tetraborate (pH = 8). After allowing the particulate material to settle to the base of the sample cup (∼ 24 h), 60 mL of supernatant was removed with a syringe and stored separately. The samples were transported in the dark at 4 °C (JGOFS Sediment Trap Methods, 1994) and stored under identical conditions upon arrival at the laboratory until further analysis. Nitrate, nitrite, ammonium and phosphate in the withdrawn supernatant were analysed colorimetrically (Aminot and Kerouel, 2007) to check for possible leaching of dissolved inorganic nitrogen and phosphorus from the particulate phase.

Samples were first transferred in a petri dish and examined under stereomicroscope (Leica MZ8, ×10 to ×50 magnification) to determine and isolate swimmers (i.e. organisms that actively entered the cup). All swimmers were carefully sorted, cleaned (rinsed with preservative solution), enumerated and removed from the cups for further taxonomic identification. As the classification of organisms as swimmers remains subjective and there is no standardized protocol, we classified zooplankton organisms as swimmers if we could observe organic material and preserved structures. Empty shells, exuvia (exoskeleton remains) and organic debris were considered part of the passive flux.

Sample preservation prevented the identification of smaller swimmers (mainly copepods) but, where possible, zooplankton were identified following Boltovskoy (1999).

Following the removal of swimmers, samples were quantitatively split into eight aliquots using a Jencons peristaltic splitter. A splitting precision of 2.9 % (coefficient of variation) was determined by weighing the particulate material obtained from each of four 1/8th aliquots (see below). Aliquots for chemical analyses were centrifuged (5 min at 3000 rpm) with the supernatant being withdrawn after this step and replaced by milliQ-grade water to remove salts. This rinsing step was repeated three times. The remaining pellet was freeze-dried (SGD-SERAIL, 0.05–0.1 mbar, −30 to 30 °C, 48 h run) and weighed three times (Sartorius MC 210 P balance, precision 10^{-4} g) to calculate the total mass. The particulate material was ground to a fine powder and used for measurements of particulate constituents.

For particulate organic carbon (POC) and particulate organic nitrogen (PON) analyses, 3 to 5 mg of the freeze-dried powder was weighed directly into pre-combusted (450 °C, 24 h) silver cups. Samples were decarbonated by adding 20 µL of 2 M analytical grade Hydrochloric acid (Sigma–Aldrich). Acidification was repeated until no bubbles could be seen, ensuring all particulate carbonate was dissolved (Salter et al., 2010). Samples were dried overnight at 50 °C. POC and PON were measured with a CHN analyzer (Perkin Elmer 2400 Series II CHNS/O Elemental Analyzer) calibrated with glycine. Samples were analysed in triplicate with an analytical precision of less than 0.7 %. Due to the small amount of particulate material in sample cups #5 and #12, replicate analyses were not possible. Uncertainty propagation for POC and PON flux was calculated as the quadratic sum of errors on mass flux and POC/PON content in each sample. The annual flux (±SD) was calculated as the sum of the time-integrated flux (±SD) in each cup.

In addition, transmissiometer (Wetlabs C-star) profiles from the KEOPS2 cruise were used to estimate POC profiles. The transmissiometer signal was calibrated against POC data (Lasbleiz et al., 2014) with the following equation: POC (μM) $= \log(\text{Xmiss}/100) \times -100.74 + 0.6401$.

3 Results

3.1 Physical conditions around trap

The sediment trap was deployed in the upper layers of Upper Circumpolar Deep Water (UCDW), beneath seasonally mixed Winter Water (WW) (Fig. 2). The depth of the CTD sensor varied between 318 and 322 m (1 and 99 % quantiles), with rare deepening to 328 m (Fig. 3a). Variations in tilt angle of the sediment trap were also low, mostly between 1 and 5°, and occasionally reaching 13° (Fig. 3d). Current speed amplitude varied between 4 and 23 $\mathrm{cm\,s^{-1}}$ (1 and 99 % quantiles) with a maximum value of 33 $\mathrm{cm\,s^{-1}}$ and a mean value of 9 $\mathrm{cm\,s^{-1}}$ (Fig. 3e). Horizontal flow vectors were divided between northward and southward components with strongest current speeds observed to flow northward (Fig. 3f and g).

The range in potential temperature and salinity was 1.85–2.23 °C and 34.12–34.26 (1–99 % quantiles) (Fig. 3b and c). From July to September 2012, a mean increase of 0.2 °C in potential temperature was associated with a strong diminution of high frequency noise suggesting a drift of the temperature sensor. Consequently these temperature data were rejected from the time-series analysis. The potential temperature/salinity diagram is compared to KEOPS1 and KEOPS2 CTD downcast at station A3 (Fig. 4). The CTD sensor recorded the signature of the UCDW and no intrusion of overlying WW could be detected.

The power spectrum of vertical sediment trap displacements identified six significant peaks corresponding to frequencies of 6.2, 8.2, 23.9, 25.7 h and 14 days (Fig. 5a). Concomitant peaks of depth, angle and current speed were also observed with a period of 14 days. However, spectral analysis of the potential density anomaly σ_θ revealed only one significant major power peak corresponding to a frequency of 12.4 h (Fig. 5b). Isopycnal displacements were driven by the unique tidal component (M2, 12.4 h period) and trap displacements resulted from a complex combination of multiple tidal components. The power spectrum analysis suggested that a 40 h window was relevant to filter out most of the short term variability (black line in Fig. 3a–e).

A pseudo-lagrangian trajectory was calculated by cumulating the instantaneous current vectors (Fig. 6). Over short time-scales (hours to day) the trajectory displays numerous tidal ellipses. The flow direction is mainly to the South-East in October 2011 to December 2012 and North-East from December 2011 to April 2012. For the entire current meter record (6 months) the overall displacement followed a 120 km northeasterly, anticlockwise trajectory with an integrated current speed of approximately 1 $\mathrm{cm\,s^{-1}}$.

3.2 Seasonality of surface chlorophyll *a* concentration above trap location

The seasonal variations of surface chlorophyll *a* concentration for the sediment trap deployment period differed significantly from the long-term climatology (Fig. 7a). The bloom started at the beginning of November 2011, ten days after the start of the sediment trap deployment. Maximum surface chlorophyll *a* values of 2.5 $\mu\mathrm{g\,L^{-1}}$ occurred on the first week of November and subsequently declined rapidly to 0.2 $\mu\mathrm{g\,L^{-1}}$ in late December 2011. A second increase in surface chlorophyll *a* up to 1 $\mu\mathrm{g\,L^{-1}}$ occurred in January 2012 and values decreased to winter levels of 0.2 $\mu\mathrm{g\,L^{-1}}$ in February 2012. A short-term increase of 0.8 $\mu\mathrm{g\,L^{-1}}$ occurred in mid-April 2012.

3.3 Swimmer abundances

No swimmers were found in cups #3 and #5 (Table 2). Total swimmer numbers were highest in winter (1544 individuals in cup #12). When normalized to cup opening time, swimmer intrusion rates were highest between mid-December 2011 and mid-February 2012 (from 26 to 55 individuals $\mathrm{d^{-1}}$) and lower than 20 individuals $\mathrm{d^{-1}}$ for the remainder of the year. Swimmers were numerically dominated by copepods throughout the year, but elevated amphipod and pteropod abundances were observed at the end of January and February 2012 (Table 2). There was no significant correlation between mass flux, POC and PON fluxes and total swimmer number or intrusion rate (Spearman's correlation test, $p > 0.01$). Copepods were essentially small cyclopoid species. Amphipods were predominantly represented by the hyperidean *Cyllopus magellanicus* and *Themisto gaudichaudii*. Pteropods were represented by *Clio pyramidata*, *Limacina helicina* forma *antarctica* and *Limacina retroversa* subsp. *australis*. Euphausiids were only represented by the genus *Thysanoessa*. One *Slapa thompsoni* salp (aggregate form) was found in the last winter cup #12.

3.4 Seasonal particulate organic carbon and nitrogen fluxes

Particulate organic carbon flux ranged from 0.15 to 0.55 $\text{mmol}\,\text{m}^{-2}\,\text{d}^{-1}$ during the productive period except during two short export events of 1.6 ± 0.04 and 1.5 ± 0.04 $\text{mmol}\,\text{m}^{-2}\,\text{d}^{-1}$ sampled in cups #4 (2 to 12 December 2011) and #9 (25 January to 8 February 2012), respectively (Fig. 7b). The two flux events occurred with an approximate time lag of one month compared to peaks in surface chlorophyll *a* values. A modest value of 0.27 ± 0.01 $\text{mmol}\,\text{m}^{-2}\,\text{d}^{-1}$ was observed in autumn (cup #11, 22 February to 30 May 2012). The lowest POC flux was measured during the winter (0.04 $\text{mmol}\,\text{m}^{-2}\,\text{d}^{-1}$, cup #12, 31 May to 7 October). Assuming that POC export was negligible from mid-September to mid-October, the annually integrated POC flux was 98.2 ± 4.4 $\text{mmol}\,\text{m}^{-2}\,\text{yr}^{-1}$ (Table 1). The two short (< 14 days) export events accounted for 16.2 ± 0.5 % (cup #4) and 21.0 ± 0.6 % (cup #9) of the annual carbon export out of the mixed layer (Table 1). Mass percentage of organic carbon ranged from 3.3 to 17.4 % (Fig. 7b). Values were slightly higher in autumn and winter (respectively 13.1 ± 0.2 % and 11 ± 2.1 % in cups #11 and #12) than in the summer, with the exception of cup #5 where the highest value of 17.4 % was observed. PON fluxes followed the same seasonal patterns as POC. This resulted in a relatively stable POC : PON ratio that varied between 6.1 to 7.4, except in the autumn cup #11 were it exceeded 8.1 (Table 1).

4 Discussion

4.1 Physical conditions of trap deployment

Moored sediment traps can be subject to hydrodynamic biases that affect the accuracy of particle collection (Buesseler et al., 2007a). The aspect ratio, tilt and horizontal flow regimes are important considerations when assessing sediment trap performance. Specifically, the line angle and aspect ratio of cylindrical traps can result in oversampling (Hawley et al., 1988). Horizontal current velocities of $12\,\mathrm{cm\,s^{-1}}$ are often invoked as a critical threshold over which particles are no longer quantitatively sampled (Baker et al., 1988). During the sediment trap deployment period we observed generally low current speeds (mean $< 10\,\mathrm{cm\,s^{-1}}$). When integrated over the entire current meter record (October 2011 to April 2012), the resulting flow is consistent with the annual northeastward, low velocity ($\sim 1\,\mathrm{cm\,s^{-1}}$) geostrophic flow previously reported over the central part of the Kerguelen plateau (Park et al., 2008b). The low current speeds, high aspect ratio of the PPS3 trap (4.75), and small mooring line angle deviations indicate the deployment was not subject to major hydrodynamic biases.

The depth of the winter mixed layer (WML) on the Kerguelen Plateau is usually shallower than 250 m (Park et al., 1998; Metzl et al., 2006). The sediment trap deployment depth of ∼ 300 m was selected to sample particle flux exiting the WML. The moored CTD sensor did not record any evidence of a winter water incursion during the deployment period, confirming the WML did not reach the trap depth. The small depth variations observed during the deployment period resulted from vertical displacement of the trap. Variations of σ_θ may have resulted from both vertical displacement of the CTD sensor and possible isopycnal displacements due to strong internal waves that can occur with an amplitude of > 50 m at this depth (Park et al., 2008a). Our measurements demonstrate that isopycnal displacements are consistent with the M2 (moon 2, 12.4 h period) tidal forcing described in physical modeling studies (Maraldi et al., 2011, 2009). Spectral analysis indicates that high frequency tidal currents are the major circulation components. Time-integrated currents shows that advection is weak and occurs over longer timescale (months). Assuming the current flow measured at the sediment trap deployment depth is representative of the prevailing current under the WML, more than three months are required for particles to leave the plateau from the A3 station, a timescale larger than the bloom duration itself. Therefore we consider that the particles collected in the sediment trap at station A3 were produced in the surface waters located above the plateau during bloom conditions.

4.2 Swimmers and particle solubilization

Aside from the hydrodynamic effects discussed above, other potential biases characterizing sediment trap deployments, particularly those in shallow waters, is the presence of swimmers and particle solubilization. Swimmers can artificially increase POC fluxes by entering the cups and releasing particulate organic matter or decrease the flux by feeding in the trap funnel (Buesseler et al., 2007a). Swimmers were most abundant in the cups #8 to #12 (January to September 2012) generally through the representation of copepods and amphipods (Table 2). Swimmer abundance was not correlated with mass flux, POC or PON fluxes, suggesting that their presence did not notably increase particulate fluxes. Nevertheless such correlations are not diagnostic and we cannot rule out the possibility of swimmer feeding in the trap funnel modifying particle flux collection during this study.

Particle solubilization in preservative solutions can lead to an underestimation of total flux measured in sediment traps. Analyses from traps poisoned with mercuric chloride suggest that ∼ 30 % of total organic carbon flux can be found in the dissolved phase and much higher values of 50 and 90 % may be observed for nitrogen and phosphorous, respectively (Antia, 2005; O'Neill et al., 2005). Unfortunately the use of a formaldehyde-based preservative in our trap samples precludes any direct estimate of excess of dissolved organic carbon in the sample cup supernatant. Furthermore, corrections for particle leaching have been considered problematic in the presence of swimmers since a fraction of the leaching may originate from the swimmers themselves (Antia, 2005), leading to over-correction. This possibly occurs in our samples since high PO_4^{3-} excess was found in the supernatant of cups where total swimmers were abundant (cups #8 to #12, data not shown). Therefore, it was impossible to accurately correct export fluxes for particle leaching. However, considering the typical leaching values for POC of 30 % reported in the literature (Antia, 2005; O'Neill et al., 2005) it is unlikely that solubilization of organic matter from passively settling particles exerts a major impact on our flux determination. Furthermore, leaching of POC should be less problematic in formalin-preserved samples because aldehydes fix organic matter, rather than just poisoning microbial activity.

4.3 Rapid flux attenuation at A3

The sediment trap record obtained from station A3 provides the first direct estimate of seasonal and annual POC export from the iron-fertilized Kerguelen bloom. The annual POC export of ~ 0.1 $\mathrm{mol\,m^{-2}\,d^{-1}}$ at ~ 300 m (Table 1) is significantly lower than indirect estimates of POC export (5.1 $\mathrm{mol\,m^{-2}\,d^{-1}}$) at the base of the WML (200 m) on the Kerguelen Plateau (Blain et al., 2007). The Kerguelen Plateau annual POC export approaches the median global ocean POC export value comprising shallow and deep sediment traps (83 $\mathrm{mmol\,m^{-2}\,yr^{-1}}$, Lampitt and Antia, 1997), but is also close to values observed in HNLC areas of the POOZ (11–43 $\mathrm{mmol\,m^{-2}\,yr^{-1}}$ at 500 m, Fischer et al., 2000). Moreover, the magnitude of annual POC export measured at ~ 300 m on the Kerguelen Plateau is comparable to deep-ocean (> 2 km) POC fluxes measured from the iron-fertilized Crozet bloom (60 $\mathrm{mmol\,m^{-2}\,d^{-1}}$, Salter et al., 2012).

The POC fluxes we measured at 300 m on the Kerguelen Plateau are low and raise some questions about possible bias in the sediment trap measurements. The current data do not seem to support a significant hydrodynamic effect in the collection of particles, but unfortunately we do not have independent radionuclide data to support this conclusion. Trap-derived particle fluxes can represent 0.1 to > 3 times the ^{234}Th-derived particles in shallow sediment traps (Buesseler, 1991; Buesseler et al., 1994; Coppola et al., 2002; Gustafsson et al., 2004) and this difference is largely attributed to the sum of hydrodynamic biases and swimmer activities (Buesseler, 1991), although it probably also includes the effect of post-collection particle solubilisation. Even if we assume that our A3 sediment trap did undersample the particle flux, it seems unlikely that this in itself could explain the significant reduction in POC flux observed between 200 and 300 m (Table 3). Although we are unable to completely eliminate the possibility of some bias in our sediment trap measurements, the coherence between our observations and independent techniques (Table 3) indicate that the rapid attenuation of flux beneath the WML is a genuine ecological feature of the Kerguelen Plateau bloom.

To further investigate the possibility of rapid flux attenuation on the Kerguelen Plateau, the sediment trap flux data were compared with parallel estimates of POC export conducted during the KEOPS2 field campaign. POC export at A3 was measured in drifting sediment traps (Laurenceau et al., 2014a), derived from ^{234}Th deficit (Planchon et al., 2014) and from particles abundances measured with an Underwater Video Profiler (UVP) (Jouandet et al., 2014). These measurements occurred during the two visits (A3-1; 20 to 21 October 2011, and A3-2; 16 November 2011) and coincided with the opening of the cups #1 and #2 of the moored sediment trap (Fig. 8). Between the 21 October and the 16 November 2011, the mean POC concentration in the mixed layer increased by almost a factor of three but remained similar at 300 m with a mean value of 3.8 µM. During the same interval, POC fluxes at 200 m derived from ^{234}Th (Planchon et al., 2014) did not change significantly. However in November, the ^{234}Th-derived POC fluxes were in the same range as 200 m UVP estimates (1.9–3.8 $\text{mmol}\,\text{m}^{-2}\,\text{d}^{-1}$) that exhibited a 13-fold increase between the two sampling dates, a fact attributed to intense algal aggregation (Jouandet et al., 2014). The POC fluxes measured in the moored sediment trap at 300 m and the UVP estimates at 350 m did not change significantly during this time. The POC fluxes observed at > 300 m by both techniques were low ($< 0.25\,\text{mmol}\,\text{m}^{-2}\,\text{d}^{-1}$) compared to the 200 m fluxes. POC fluxes in the third sampling cup (open until beginning of December) were also low (0.15 $\text{mmol}\,\text{m}^{-2}\,\text{d}^{-1}$, Table 1).

The daily POC export fluxes measured at A3 by the moored sediment trap were also compared with 2005 summer cruise flux estimates measured during KEOPS1

(Table 3). The diversity of approaches prevents absolute comparison of the fluxes, however there are several notable trends. The measurement of these fluxes at the end of the 2005 bloom is concomitant with the highest recorded POC fluxes measured by the A3 sediment trap during the 2011 bloom (Fig. 7b). Most of these previous estimates were made at depths < 200 m and are one to two orders of magnitude greater than the maximum observed A3 sediment trap flux (~ 300 m) of 1.6 mmol m^{-2} d^{-1} measured in December (Table 1). Similarly low estimates of 0.7 and 1 mmol m^{-2} d^{-1} were measured during KEOPS1 in drifting gel traps at 330 and 430 m, respectively (Ebersbach and Trull, 2008). Therefore, rapid flux attenuation beneath the base of the WML (200 m) appears to be a feature observed during both spring and summer periods.

To constrain the magnitude of flux attenuation, 200 and 300 m POC fluxes during spring and summer were compared using a power-law curve (Martin et al., 1987). A classical range for the *b* exponant (0.4 to 1.7) is equivalent to a reduction in POC flux between 200 and 300 m of ~ 15–55 %. Here we used the ^{234}Th fluxes (Planchon et al., 2014) and UVP estimates (Jouandet et al., 2014) at 200 m in spring and ^{234}Th fluxes (Savoye et al., 2008) and drifting gel trap estimates (Ebersbach and Trull, 2008) at 200 m in summer, with the congruent POC fluxes from the A3 moored sediment trap at 289 m. The calculation yields *b* values of 7–11.3, which equates POC flux attenuation of 94–96 % over a 100 m depth interval. These estimates from spring and summer are comparable with the 98 % reduction in POC flux from 5.1 mol m^{-2} yr^{-1} at 200 m (Blain et al., 2007) to 0.1 mol m^{-2} yr^{-1} (this study) inferred from the comparison of annual flux budgets over the same depth interval. There is therefore consistent evidence supporting rapid flux attenuation at the base of the WML over the Kerguelen Plateau during the period of major annual bloom transfer to the sediments.

4.4 Hypotheses for rapid flux attenuation

The annual export of POC at 289 m is exceptionally low (98.2 ± 4.4 mmol m^{-2} yr^{-1}) compared to estimates of seasonal net community carbon production (6.6 ± 2.2 mol m^{-2}; Jouandet et al., 2008) and estimates of POC export at the base of the

WML (5.1 mol m^{-2}; Blain et al., 2007). Retention and degradation of particulate material above the WML (220 m) may partially explain the strong flux attenuation within and below the WML. The POC : PON ratio measured in the trap material is close to the Redfield value for phytoplankton of 6.6 (Redfield, 1934) in spring and summer, implying a significant contribution of phytoplanktonic cells to the exported material, which is corroborated by detailed microscopic analysis (Rembauville et al., 2014). Sinking speed can vary from 1 m d^{-1} for single phytoplankton cells to ∼ 100 m d^{-1} for phytoaggregates (Allredge and Gotschalk, 1988; Peterson et al., 2005; Trull et al., 2008a) and can reach values > 2000 m d^{-1} for large fecal pellets (Turner, 2002). Given the shallow trap depth (289 m), export via phytoaggregates following bloom demise would suggest a short lag of a few days between the bloom peak (Fig. 7) and flux peaks (cf. Turner, 2002; Honda et al., 2006; Trull et al., 2008a; Laurenceau et al., 2014b). However, the temporal lag measured in our study is approximately one month, implying either slow settling rates characterstic of single cells or faster settling fluxes that do not originate from the peak in surface production. Slow sinking rates between surface production and export and may be a causal factor for the strong attenuation by allowing particles to be remineralized in the mixed layer and/or intercepted by higher trophic levels.

The remineralization of particles by heterotrophic microbes is unlikely to completely account for this reduction in POC flux. In summer, the bacterial carbon production (BP) at 200 m at station A3 is approximately 10 nmol L^{-1} d^{-1} and bacterial growth efficiency (BGE) ranges between 8–15 % (Obernosterer et al., 2008). Calculating the bacterial carbon demand (BCD = BP/BGE) and integrating it between 200 and 289 m suggests that a POC flux attenuation in the range of 5.9 to 11.1 mmol m^{-2} d^{-1} could be reasonably attributed to heterotrophic microbial activity. Although significant, this estimate cannot account for the difference between the POC flux at 200 and 289 m (e.g. 22.9 mmol m^{-2} d^{-1} attenuation from 24.5 to 1.6 mmol m^{-2} d^{-1} in summer; Table 3). Furthermore, these values are likely to be an overestimate because they imply bacterial production is exclusively controlled by particulate organic carbon and ignore the important role of dissolved carbon substrates. The Barium excess (Ba$_{xs}$) proxy provides an alternative estimate of carbon remineralization (Dehairs et al., 1997). Carbon remineralization rates integrated over 150–400 m are equal to 0.9–1.2 mmol $m^{-2} d^{-1}$ in spring (Jacquet et al., 2014) and 2.1–2.8 mmol $m^{-2} d^{-1}$ in summer (Jacquet et al., 2008). These remineralisation rates are also too low to explain the observed attenuation in POC flux at the base of the mixed layer.

Based on the available data we invoke the role of higher trophic levels in flux attenuation. Mesozooplankton biomass and community structure is reported for the A3 station in spring and summer in Carlotti et al. (2008, 2014). Between October and November 2011, mesozooplankton biomass in the mixed layer doubled (Carlotti et al., 2014). In summer (January 2005), the observed mesozooplankton biomass was again twofold higher than in spring 2011 (Carlotti et al., 2008). It was concluded that the zooplankton community structure was able to answer more rapidly to phytoplankton biomass availability on the plateau compared to oceanic water, leading to higher secondary production on the plateau (Carlotti et al., 2008, 2014). Efficient grazers such as *Oithona similis* (McLeod et al., 2010; Pinkerton et al., 2010), that also exhibit coprophagy, may increase carbon retention in higher trophic compartments (Gonzalez and Smetacek, 1994). Furthemore, it is possible that vertical migrating zooplankton communities produce fecal pellets below the trap deployment depth. Notably, *Oithona similis* represents > 50 % of the mesozooplankton assemblage at the station A3 in spring (Carlotti et al., 2014) whereas the summer community structure is more diversified, containing small copepods but also larger calanoid copepods, pteropods and amphipods (Carlotti et al., 2008). This is consistent with the maximum swimmer intrusion rate and swimmer diversity observed in summer (Table 2). A recent study in the North Pacific supports the significance of mesopelagic fish communities for carbon flux attenuation (Davison et al., 2013). Although important for carbon budgets it is a compartment often neglected due to the challenge of quantitative sampling approaches. Mesopelagic fish larvae are known to be abundant on the southern part of the Kerguelen plateau (myctophid spawning and larvae foraging site, Koubbi et al., 1991, 2001). We offer the hypothesis that a significant fraction of net community production is channeled to higher trophic levels through mesozooplankton dynamics and possibly myctophid fishes that fuel large mammal and bird populations around the Plateau. Therefore high grazing pressure and an efficient shift of carbon biomass to predatory mammals and birds may be responsible for the HBLE scenario encountered on the productive iron-fertilized Kerguelen Plateau.

5 Conclusions

We have reported the seasonal dynamics of particulate organic carbon (POC) export under the winter mixed layer (289 m) of the naturally fertilized, productive central Kerguelen Plateau. Annual POC flux was very low (98 mmol m^{-2}) and most of it occurred during two episodic (< 14 days) events exported with a 1 month lag following two surface chlorophyll *a* peaks. Analysis of the hydrological conditions did not support strong hydrodynamic biases that could explain the low fluxes observed. A comparison with different estimates of POC fluxes in spring and summer at the same station allowed to identify a strong flux attenuation between the basis of the mixed layer and the sediment trap depth. Bacterial heterotrophic activity in the upper mesopelagic is not enough to explain the observed attenuation. We invoke mesozooplankton and possibly mesopelagic fishes activity for being responsible for efficient the carbon retention and/or transfer to higher trophic levels in, or at the basis, of the mixed layer as a possible explanation for the HBLE scenario observed.

The biogenic silicon, diatoms and faecal pellet fluxes are reported in a companion paper that aims to identify the ecological vectors that explain the intensity and the BSi:POC ratio of the fluxes (Rembauville et al., 2014).

Acknowledgements. We thank the Chief Scientist Bernard Quéguiner, the Captain Bernard Lassiette and his crew during the KEOPS2 mission on the R/V *Marion Dufresne II*. We thank Leanne Armand and Tom Trull for their constructive comments, which helped us to improve the manuscript. This work was supported by the French Research program of INSU-CNRS LEFE-CYBER (Les enveloppes fluides et l'environnement – Cycles biogéochimiques, environnement et ressources), the French ANR (Agence Nationale de la Recherche, SIMI-6 program, ANR-10-BLAN-0614), the French CNES (Centre National d'Etudes Spatiales) and the French Polar Institute IPEV (Institut Polaire Paul-Emile Victor).

References

Allredge, A. L. and Gotschalk, C.: In situ settling behavior of marine snow, Limnol. Oceanogr., 33, 339–351, 1988.

Aminot, A. and Kerouel, R.: Dosage automatique des nutriments dans les eaux marines: meìthodes en flux continu, Ifremer, Plouzaneì, France, 2007.

Antia, A. N.: Solubilization of particles in sediment traps: revising the stoichiometry of mixed layer export, Biogeosciences, 2, 189–204, doi:10.5194/bg-2-189-2005, 2005.

Arrigo, K. R., Worthen, D., Schnell, A., and Lizotte, M. P.: Primary production in Southern Ocean waters, J. Geophys. Res.-Oceans, 103, 15587–15600, doi:10.1029/98JC00930, 1998.

Baker, E. T., Milburn, H. B., and Tennant, D. A.: Field assessment of sediment trap efficiency under varying flow conditions, J. Mar. Res., 46, 573–592, doi:10.1357/002224088785113522, 1988.

Barbeau, K., Moffett, J. W., Caron, D. A., Croot, P. L., and Erdner, D. L.: Role of protozoan grazing in relieving iron limitation of phytoplankton, Nature, 380, 61–64, doi:10.1038/380061a0, 1996.

Batten, S. D. and Gower, J. F. R.: Did the iron fertilization near Haida Gwaii in 2012 affect the pelagic lower trophic level ecosystem?, J. Plankton Res., 36, 925–932, 2014.

Blain, S., Tréguer, P., Belviso, S., Bucciarelli, E., Denis, M., Desabre, S., Fiala, M., Martin Jézéquel, V., Le Fèvre, J., Mayzaud, P., Marty, J.-C., and Razouls, S.: A biogeochemical study of the island mass effect in the context of the iron hypothesis: Kerguelen Islands, Southern Ocean, Deep-Sea Res., 48, 163–187, doi:10.1016/S0967-0637(00)00047-9, 2001.

Blain, S., Quéguiner, B., Armand, L., Belviso, S., Bombled, B., Bopp, L., Bowie, A., Brunet, C., Brussaard, C., Carlotti, F., Christaki, U., Corbière, A., Durand, I., Ebersbach, F., Fuda, J.-L., Garcia, N., Gerringa, L., Griffiths, B., Guigue, C., Guillerm, C., Jacquet, S., Jeandel, C., Laan, P., Lefèvre, D., Lo Monaco, C., Malits, A., Mosseri, J., Obernosterer, I., Park, Y.-H., Picheral, M., Pondaven, P., Remenyi, T., Sandroni, V., Sarthou, G., Savoye, N., Scouarnec, L., Souhaut, M., Thuiller, D., Timmermans, K., Trull, T., Uitz, J., van Beek, P., Veldhuis, M., Vincent, D., Viollier, E., Vong, L., and Wagener, T.: Effect of natural iron fertilization on carbon sequestration in the Southern Ocean, Nature, 446, 1070–1074, doi:10.1038/nature05700, 2007.

Boltovskoy, D.: South Atlantic Zooplankton, Backhuys, 1999.

Bopp, L., Kohfeld, K. E., Le Quéré, C., and Aumont, O.: Dust impact on marine biota and atmospheric CO_2 during glacial periods, Paleoceanography, 18, 1046, doi:10.1029/2002PA000810, 2003.

Boyd, P. W. and Trull, T. W.: Understanding the export of biogenic particles in oceanic waters: is there consensus?, Prog. Oceanogr., 72, 276–312, doi:10.1016/j.pocean.2006.10.007, 2007.

Boyd, P. W., Law, C. S., Hutchins, D. A., Abraham, E. R., Croot, P. L., Ellwood, M., Frew, R. D., Hadfield, M., Hall, J., Handy, S., Hare, C., Higgins, J., Hill, P., Hunter, K. A., LeBlanc, K., Maldonado, M. T., McKay, R. M., Mioni, C., Oliver, M., Pickmere, S., Pinkerton, M., Safi, K., Sander, S., Sanudo-Wilhelmy, S. A., Smith, M., Strzepek, R., Tovar-Sanchez, A., and Wilhelm, S. W.: FeCycle: attempting an iron biogeochemical budget from a mesoscale SF6 tracer experiment in unperturbed low iron waters, Global Biogeochem. Cy., 19, GB4S20, doi:10.1029/2005GB002494, 2005.

Boyd, P. W., Jickells, T., Law, C. S., Blain, S., Boyle, E. A., Buesseler, K. O., Coale, K. H., Cullen, J. J., Baar, H. J. W. de, Follows, M., Harvey, M., Lancelot, C., Levasseur, M., Owens, N. P. J., Pollard, R., Rivkin, R. B., Sarmiento, J., Schoemann, V., Smetacek, V., Takeda, S., Tsuda, A., Turner, S., and Watson, A. J.: Mesoscale iron enrichment experiments 1993–2005: synthesis and future directions, Science, 315, 612–617, doi:10.1126/science.1131669, 2007.

Buesseler, K. O.: Do upper-ocean sediment traps provide an accurate record of particle flux?, Nature, 353, 420–423, doi:10.1038/353420a0, 1991.

Buesseler, K. O. and Boyd, P. W.: Shedding light on processes that control particle export and flux attenuation in the twilight zone of the open ocean, Limnol. Oceanogr., 54, 1210–1232, doi:10.4319/lo.2009.54.4.1210, 2009.

Buesseler, K. O., Michaels, A. F., Siegel, D. A., and Knap, A. H.: A three dimensional time-dependent approach to calibrating sediment trap fluxes, Global Biogeochem. Cy., 8, 179–193, doi:10.1029/94GB00207, 1994.

Buesseler, K. O., Benitez-Nelson, C. R., Moran, S. B., Burd, A., Charette, M., Cochran, J. K., Coppola, L., Fisher, N. S., Fowler, S. W., Gardner, W. D., Guo, L. D., Gustafsson, Ö., Lamborg, C., Masque, P., Miquel, J. C., Passow, U., Santschi, P. H., Savoye, N., Stewart, G., and Trull, T.: An assessment of particulate organic carbon to thorium-234 ratios in the ocean and their impact on the application of ^{234}Th as a POC flux proxy, Future Applications of ^{234}Th in Aquatic Ecosystems (FATE), Mar. Chem., 100, 213–233, doi:10.1016/j.marchem.2005.10.013, 2006.

Buesseler, K. O., Antia, A. N., Chen, M., Fowler, S. W., Gardner, W. D., Gustafsson, Ö., Harada, K., Michaels, A. F., Rutgers v. d. Loeff, M., Sarin, M., Steinberg, D. K., and Trull, T.: An assessment of the use of sediment traps for estimating upper ocean particle fluxes, J. Mar. Res., 65, 345–416, 2007a.

Buesseler, K. O., Lamborg, C. H., Boyd, P. W., Lam, P. J., Trull, T. W., Bidigare, R. R., Bishop, J. K. B., Casciotti, K. L., Dehairs, F., Elskens, M., Honda, M., Karl, D. M., Siegel, D. A., Silver, M. W., Steinberg, D. K., Valdes, J., Mooy, B. V., and Wilson, S.: Revisiting carbon flux through the ocean's twilight zone, Science, 316, 567–570, doi:10.1126/science.1137959, 2007b.

Carlotti, F., Thibault-Botha, D., Nowaczyk, A., and Lefèvre, D.: Zooplankton community structure, biomass and role in carbon fluxes during the second half of a phytoplankton bloom in the eastern sector of the Kerguelen Shelf (January–February 2005), Deep-Sea Res. Pt. II, 55, 720–733, doi:10.1016/j.dsr2.2007.12.010, 2008.

Carlotti, F., Jouandet, M.-P., Nowaczyk, A., Harmelin-Vivien, M., Lefèvre, D., Guillou, G., Zhu, Y., and Zhou, M.: Mesozooplankton structure and functioning during the onset of the Kerguelen Bloom during KEOPS2 survey, Biogeosciences, in preparation, 2014.

Coale, K. H. and Bruland, K. W.: ^{234}Th:^{238}U disequilibria within the california current, Limnol. Oceanogr., 30, 22–33, 1985.

Coale, K. H., Johnson, K. S., Chavez, F. P., Buesseler, K. O., Barber, R. T., Brzezinski, M. A., Cochlan, W. P., Millero, F. J., Falkowski, P. G., Bauer, J. E., Wanninkhof, R. H., Kudela, R. M., Altabet, M. A., Hales, B. E., Takahashi, T., Landry, M. R., Bidigare, R. R., Wang, X., Chase, Z., Strutton, P. G., Friederich, G. E., Gorbunov, M. Y., Lance, V. P., Hilting, A. K., Hiscock, M. R., Demarest, M., Hiscock, W. T., Sullivan, K. F., Tanner, S. J., Gordon, R. M., Hunter, C. N., Elrod, V. A., Fitzwater, S. E., Jones, J. L., Tozzi, S., Koblizek, M., Roberts, A. E., Herndon, J., Brewster, J., Ladizinsky, N., Smith, G., Cooper, D., Timothy, D., Brown, S. L., Selph, K. E., Sheridan, C. C., Twining, B. S., and Johnson, Z. I.: Southern ocean iron enrichment experiment: carbon cycling in high- and low-Si waters, Science, 304, 408–414, doi:10.1126/science.1089778, 2004.

Coppola, L., Roy-Barman, M., Wassmann, P., Mulsow, S., and Jeandel, C.: Calibration of sediment traps and particulate organic carbon export using ^{234}Th in the Barents Sea, Mar. Chem., 80, 11–26, doi:10.1016/S0304-4203(02)00071-3, 2002.

Davison, P. C., Checkley Jr., D. M., Koslow, J. A., and Barlow, J.: Carbon export mediated by mesopelagic fishes in the northeast Pacific Ocean, Prog. Oceanogr., 116, 14–30, doi:10.1016/j.pocean.2013.05.013, 2013.

De Baar, H. J. W., Buma, A. G. J., Nolting, R. F., Cadée, G. C., Jacques, G., and Tréguer, P.: On iron limitation of the Southern Ocean: experimental observations in the Weddell and Scotia Seas, Mar. Ecol.-Prog. Ser., 65, 105–122, doi:10.3354/meps065105, 1990.

De Baar, H. J. W., Boyd, P. W., Coale, K. H., Landry, M. R., Tsuda, A., Assmy, P., Bakker, D. C. E., Bozec, Y., Barber, R. T., Brzezinski, M. A., Buesseler, K. O., Boyé, M., Croot, P. L., Gervais, F., Gorbunov, M. Y., Harrison, P. J., Hiscock, W. T., Laan, P., Lancelot, C., Law, C. S., Levasseur, M., Marchetti, A., Millero, F. J., Nishioka, J., Nojiri, Y., van Oijen, T., Riebesell, U., Rijkenberg, M. J. A., Saito, H., Takeda, S., Timmermans, K. R., Veldhuis, M. J. W., Waite, A. M., and Wong, C.-S.: Synthesis of iron fertilization experiments: from the iron age in the age of enlightenment, J. Geophys. Res.-Oceans, 110, C09S16, doi:10.1029/2004JC002601, 2005.

Dehairs, F., Shopova, D., Ober, S., Veth, C., and Goeyens, L.: Particulate barium stocks and oxygen consumption in the Southern Ocean mesopelagic water column during spring and early summer: relationship with export production, Deep-Sea Res. Pt. II, 44, 497–516, doi:10.1016/S0967-0645(96)00072-0, 1997.

Dilling, L. and Alldredge, A. L.: Fragmentation of marine snow by swimming macrozooplankton: a new process impacting carbon cycling in the sea, Deep-Sea Res., 47, 1227–1245, doi:10.1016/S0967-0637(99)00105-3, 2000.

Dunne, J. P., Sarmiento, J. L., and Gnanadesikan, A.: A synthesis of global particle export from the surface ocean and cycling through the ocean interior and on the seafloor, Global Biogeochem. Cy., 21, GB4006, doi:10.1029/2006GB002907, 2007.

Ebersbach, F. and Trull, T. W.: Sinking particle properties from polyacrylamide gels during the KErguelen Ocean and Plateau compared Study (KEOPS): zooplankton control of carbon export in an area of persistent natural iron inputs in the Southern Ocean, Limnol. Oceanogr., 53, 212–224, doi:10.4319/lo.2008.53.1.0212, 2008.

Ebersbach, F., Trull, T. W., Davies, D. M., and Bray, S. G.: Controls on mesopelagic particle fluxes in the Sub-Antarctic and Polar Frontal Zones in the Southern Ocean south of Australia in summer – perspectives from free-drifting sediment traps, Deep-Sea Res. Pt. II, 58, 2260–2276, doi:10.1016/j.dsr2.2011.05.025, 2011.

Fischer, G., Ratmeyer, V., and Wefer, G.: Organic carbon fluxes in the Atlantic and the Southern Ocean: relationship to primary production compiled from satellite radiometer data, Deep-Sea Res. Pt. II, 47, 1961–1997, doi:10.1016/S0967-0645(00)00013-8, 2000.

Francois, R., Honjo, S., Krishfield, R., and Manganini, S.: Factors controlling the flux of organic carbon to the bathypelagic zone of the ocean, Global Biogeochem. Cy., 16, 1087, doi:10.1029/2001GB001722, 2002.

Gall, M. P., Strzepek, R., Maldonado, M., and Boyd, P. W.: Phytoplankton processes, Part 2: Rates of primary production and factors controlling algal growth during the Southern Ocean Iron RElease Experiment (SOIREE), the Southern Ocean Iron Release Experiment (SOIREE), Deep-Sea Res. Pt. II, 48, 2571–2590, doi:10.1016/S0967-0645(01)00009-1, 2001.

Gehlen, M., Bopp, L., Emprin, N., Aumont, O., Heinze, C., and Ragueneau, O.: Reconciling surface ocean productivity, export fluxes and sediment composition in a global biogeochemical ocean model, Biogeosciences, 3, 521–537, doi:10.5194/bg-3-521-2006, 2006.

Giering, S. L. C., Sanders, R., Lampitt, R. S., Anderson, T. R., Tamburini, C., Boutrif, M., Zubkov, M. V., Marsay, C. M., Henson, S. A., Saw, K., Cook, K., and Mayor, D. J.: Reconciliation of the carbon budget in the ocean's twilight zone, Nature, advance online publication, 507, 480–483, 2014.

Gilman, D. L., Fuglister, F. J., and Mitchell, J. M.: On the power spectrum of "Red Noise", J. Atmos. Sci., 20, 182–184, doi:10.1175/1520-0469(1963)020<0182:OTPSON>2.0.CO;2, 1963.

Gonzalez, H. E. and Smetacek, V.: The possible role of the cyclopoid copepod Oithona in retarding vertical flux of zooplankton faecal material, Mar. Ecol.-Prog. Ser., 113, 233–246, 1994.

Gruber, N., Gloor, M., Mikaloff Fletcher, S. E., Doney, S. C., Dutkiewicz, S., Follows, M. J., Gerber, M., Jacobson, A. R., Joos, F., Lindsay, K., Menemenlis, D., Mouchet, A., Müller, S. A., Sarmiento, J. L., and Takahashi, T.: Oceanic sources, sinks, and transport of atmospheric CO_2, Global Biogeochem. Cy., 23, GB1005, doi:10.1029/2008GB003349, 2009.

Gustafsson, O., Andersson, P., Roos, P., Kukulska, Z., Broman, D., Larsson, U., Hajdu, S., and Ingri, J.: Evaluation of the collection efficiency of upper ocean sub-photic-layer sediment traps: a 24 month in situ calibration in the open Baltic Sea using ^{234}Th, Limnol. Oceanogr.-Meth., 2, 62–74, doi:10.4319/lom.2004.2.62, 2004.

Henson, S. A., Sanders, R., Madsen, E., Morris, P. J., Le Moigne, F., and Quartly, G. D.: A reduced estimate of the strength of the ocean's biological carbon pump, Geophys. Res. Lett., 38, L04606, doi:10.1029/2011GL046735, 2011.

Henson, S. A., Sanders, R., and Madsen, E.: Global patterns in efficiency of particulate organic carbon export and transfer to the deep ocean, Global Biogeochem. Cy., 26, GB1028, doi:10.1029/2011GB004099, 2012.

Hiscock, W. T. and Millero, F. J.: Nutrient and carbon parameters during the Southern Ocean iron experiment (SOFeX), Deep-Sea Res., 52, 2086–2108, doi:10.1016/j.dsr.2005.06.010, 2005.

Honda, M. C., Kawakami, H., Sasaoka, K., Watanabe, S., and Dickey, T.: Quick transport of primary produced organic carbon to the ocean interior, Geophys. Res. Lett., 33, L16603, doi:10.1029/2006GL026466, 2006.

Honjo, S., Manganini, S. J., Krishfield, R. A., and Francois, R.: Particulate organic carbon fluxes to the ocean interior and factors controlling the biological pump: a synthesis of global sediment trap programs since 1983, Prog. Oceanogr., 76, 217–285, doi:10.1016/j.pocean.2007.11.003, 2008.

Hudson, J. M., Steinberg, D. K., Sutton, T. T., Graves, J. E., and Latour, R. J.: Myctophid feeding ecology and carbon transport along the northern mid-Atlantic ridge, Deep-Sea Res., 93, 104–116, 2014.

Jacquet, S. H. M., Dehairs, F., Savoye, N., Obernosterer, I., Christaki, U., Monnin, C., and Cardinal, D.: Mesopelagic organic carbon remineralization in the Kerguelen Plateau region tracked by biogenic particulate Ba, Deep-Sea Res. Pt. II, 55, 868–879, doi:10.1016/j.dsr2.2007.12.038, 2008.

JGOFS Sediment Trap Methods: Protocols for the Joint Global Ocean Flux Study (JGOFS) Core Measurements, Intergovernmental Oceanographic Commission, Scientific Committee on Oceanic Research Manual and Guides, UNESCO, 157–164, 1994.

Jouandet, M. P., Blain, S., Metzl, N., Brunet, C., Trull, T. W., and Obernosterer, I.: A seasonal carbon budget for a naturally iron-fertilized bloom over the Kerguelen Plateau in the Southern Ocean, KEOPS: Kerguelen Ocean and Plateau compared Study, Deep-Sea Res. Pt. II, 55, 856–867, doi:10.1016/j.dsr2.2007.12.037, 2008.

Jouandet, M.-P., Trull, T. W., Guidi, L., Picheral, M., Ebersbach, F., Stemmann, L., and Blain, S.: Optical imaging of mesopelagic particles indicates deep carbon flux beneath a natural iron-fertilized bloom in the Southern Ocean, Limnol. Oceanogr., 56, 1130–1140, doi:10.4319/lo.2011.56.3.1130, 2011.

Jouandet, M.-P., Jackson, G. A., Carlotti, F., Picheral, M., Stemmann, L., and Blain, S.: Rapid formation of large aggregates during the spring bloom of Kerguelen Island: observations and model comparisons, Biogeosciences, 11, 4393–4406, doi:10.5194/bg-11-4393-2014, 2014.

Karleskind, P., Lévy, M., and Memery, L.: Subduction of carbon, nitrogen, and oxygen in the northeast Atlantic, J. Geophys. Res.-Oceans, 116, C02025, doi:10.1029/2010JC006446, 2011.

Kohfeld, K. E., Quéré, C. L., Harrison, S. P., and Anderson, R. F.: Role of marine biology in glacial–interglacial CO_2 cycles, Science, 308, 74–78, doi:10.1126/science.1105375, 2005.

Korb, R. E. and Whitehouse, M.: Contrasting primary production regimes around South Georgia, Southern Ocean: large blooms vs. high nutrient, low chlorophyll waters, Deep-Sea Res., 51, 721–738, doi:10.1016/j.dsr.2004.02.006, 2004.

Koubbi, P., Duhamel, G., and Hebert, C.: Seasonal relative abundance of fish larvae inshore at Îles Kerguelen, Southern Ocean, Antarct. Sci., 13, 385–392, doi:10.1017/S0954102001000542, 2001.

Koubbi, P., Ibanez, F., and Duhamel, G.: Environmental influences on spatio-temporal oceanic distribution of ichthyoplankton around the Kerguelen Islands (Southern Ocean), Mar. Ecol.-Prog. Ser., 72, 225–238, 1991.

Lam, P. J. and Bishop, J. K. B.: High biomass, low export regimes in the Southern Ocean, Deep-Sea Res. Pt. II, 54, 601–638, doi:10.1016/j.dsr2.2007.01.013, 2007.

Lam, P. J., Doney, S. C., and Bishop, J. K. B.: The dynamic ocean biological pump: insights from a global compilation of particulate organic carbon, $CaCO_3$, and opal concentration profiles from the mesopelagic, Global Biogeochem. Cy., 25, GB3009, doi:10.1029/2010GB003868, 2011.

Lampitt, R. S. and Antia, A. N.: Particle flux in deep seas: regional characteristics and temporal variability, Deep-Sea Res., 44, 1377–1403, doi:10.1016/S0967-0637(97)00020-4, 1997.

Lampitt, R. S., Boorman, B., Brown, L., Lucas, M., Salter, I., Sanders, R., Saw, K., Seeyave, S., Thomalla, S. J., and Turnewitsch, R.: Particle export from the euphotic zone: estimates using a novel drifting sediment trap, ^{234}Th and new production, Deep-Sea Res., 55, 1484–1502, doi:10.1016/j.dsr.2008.07.002, 2008.

Landry, M. R., Constantinou, J., Latasa, M., Brown, S. L., Bidigare, R. R., and Ondrusek, M. E.: Biological response to iron fertilization in the eastern equatorial Pacific (IronEx II). III. Dynamics of phytoplankton growth and microzooplankton grazing, Mar. Ecol.-Prog. Ser., 201, 57–72, doi:10.3354/meps201057, 2000.

Lasbleiz, M., Leblanc, K., Blain, S., Ras, J., Cornet-Barthaux, V., Hélias Nunige, S., and Quéguiner, B.: Pigments, elemental composition (C, N, P, and Si), and stoichiometry of particulate matter in the naturally iron fertilized region of Kerguelen in the Southern Ocean, Biogeosciences, 11, 5931–5955, doi:10.5194/bg-11-5931-2014, 2014.

Laurenceau, E. C., Trull, T. W., Davies, D. M., Bray, S. G., Doran, J., Planchon, F., Carlotti, F., Jouandet, M.-P., Cavagna, A.-J., Waite, A. M., and Blain, S.: The relative importance of phytoplankton aggregates and zooplankton fecal pellets to carbon export: insights from free-drifting sediment trap deployments in naturally iron-fertilised waters near the Kerguelen plateau, Biogeosciences Discuss., 11, 13623–13673, doi:10.5194/bgd-11-13623-2014, 2014a.

Laurenceau, E. C., Trull, T. W., Davies, D., De La Rocha, C. L., and and Blain, S.: Phytoplankton morphology controls on marine snow sinking velocity, Mar. Ecol.-Prog. Ser., in review, 2014b.

Laws, E. A., Falkowski, P. G., Smith, W. O., Ducklow, H., and McCarthy, J. J.: Temperature effects on export production in the open ocean, Global Biogeochem. Cy., 14, 1231–1246, doi:10.1029/1999GB001229, 2000.

Laws, E. A., D'Sa, E., and Naik, P.: Simple equations to estimate ratios of new or export production to total production from satellite-derived estimates of sea surface temperature and primary production, Limnol. Oceanogr.-Meth., 9, 593–601, doi:10.4319/lom.2011.9.593, 2011.

Lefèvre, D., Guigue, C., and Obernosterer, I.: The metabolic balance at two contrasting sites in the Southern Ocean: the iron-fertilized Kerguelen area and HNLC waters, KEOPS: Kerguelen Ocean and Plateau compared Study, Deep-Sea Res. Pt. II, 55, 766–776, doi:10.1016/j.dsr2.2007.12.006, 2008.

Le Moigne, F. A. C., Sanders, R. J., Villa-Alfageme, M., Martin, A. P., Pabortsava, K., Planquette, H., Morris, P. J., and Thomalla, S. J.: On the proportion of ballast vs. non-ballast associated carbon export in the surface ocean, Geophys. Res. Lett., 39, L15610, doi:10.1029/2012GL052980, 2012.

Lenton, A., Tilbrook, B., Law, R. M., Bakker, D., Doney, S. C., Gruber, N., Ishii, M., Hoppema, M., Lovenduski, N. S., Matear, R. J., McNeil, B. I., Metzl, N., Mikaloff Fletcher, S. E., Monteiro, P. M. S., Rödenbeck, C., Sweeney, C., and Takahashi, T.: Sea–air CO_2 fluxes in the Southern Ocean for the period 1990–2009, Biogeosciences, 10, 4037–4054, doi:10.5194/bg-10-4037-2013, 2013.

Le Quéré, C., Andres, R. J., Boden, T., Conway, T., Houghton, R. A., House, J. I., Marland, G., Peters, G. P., van der Werf, G. R., Ahlström, A., Andrew, R. M., Bopp, L., Canadell, J. G., Ciais, P., Doney, S. C., Enright, C., Friedlingstein, P., Huntingford, C., Jain, A. K., Jourdain, C., Kato, E., Keeling, R. F., Klein Goldewijk, K., Levis, S., Levy, P., Lomas, M., Poulter, B., Raupach, M. R., Schwinger, J., Sitch, S., Stocker, B. D., Viovy, N., Zaehle, S., and Zeng, N.: The global carbon budget 1959–2011, Earth Syst. Sci. Data, 5, 165–185, doi:10.5194/essd-5-165-2013, 2013.

Levy, M., Bopp, L., Karleskind, P., Resplandy, L., Ethe, C., and Pinsard, F.: Physical pathways for carbon transfers between the surface mixed layer and the ocean interior, Global Biogeochem. Cy., 27, 1001–1012, doi:10.1002/gbc.20092, 2013.

Lima, I. D., Lam, P. J., and Doney, S. C.: Dynamics of particulate organic carbon flux in a global ocean model, Biogeosciences, 11, 1177–1198, doi:10.5194/bg-11-1177-2014, 2014.

Lutz, M. J., Caldeira, K., Dunbar, R. B., and Behrenfeld, M. J.: Seasonal rhythms of net primary production and particulate organic carbon flux to depth describe the efficiency of biological pump in the global ocean, J. Geophys. Res.-Oceans, 112, C10011, doi:10.1029/2006JC003706, 2007.

Maiti, K., Charette, M. A., Buesseler, K. O., and Kahru, M.: An inverse relationship between production and export efficiency in the Southern Ocean, Geophys. Res. Lett., 40, 1557–1561, doi:10.1002/grl.50219, 2013.

Maraldi, C., Mongin, M., Coleman, R., and Testut, L.: The influence of lateral mixing on a phytoplankton bloom: distribution in the Kerguelen Plateau region, Deep-Sea Res., 56, 963–973, doi:10.1016/j.dsr.2008.12.018, 2009.

Maraldi, C., Lyard, F., Testut, L., and Coleman, R.: Energetics of internal tides around the Kerguelen Plateau from modeling and altimetry, J. Geophys. Res.-Oceans, 116, C06004, doi:10.1029/2010JC006515, 2011.

Maritorena, S. and Siegel, D. A.: Consistent merging of satellite ocean color data sets using a bio-optical model, Remote Sens. Environ., 94, 429–440, doi:10.1016/j.rse.2004.08.014, 2005.

Martin, J. H., Knauer, G. A., Karl, D. M., and Broenkow, W. W.: VERTEX: carbon cycling in the northeast Pacific, Deep-Sea Res., 34, 267–285, doi:10.1016/0198-0149(87)90086-0, 1987.

Martin, P., van der Loeff, M. R., Cassar, N., Vandromme, P., d' Ovidio, F., Stemmann, L., Rengarajan, R., Soares, M., González, H. E., Ebersbach, F., Lampitt, R. S., Sanders, R., Barnett, B. A., Smetacek, V., and Naqvi, S. W. A.: Iron fertilization enhanced net community production but not downward particle flux during the Southern Ocean iron fertilization experiment LOHAFEX, Global Biogeochem. Cy., 27, 871–881, doi:10.1002/gbc.20077, 2013.

McLeod, D. J., Hosie, G. W., Kitchener, J. A., Takahashi, K. T., and Hunt, B. P. V.: Zooplankton atlas of the southern ocean: the SCAR SO-CPR survey (1991–2008), Antarctic biology in the 21st century – advances in and beyond IPY, Polar Sci., 4, 353–385, doi:10.1016/j.polar.2010.03.004, 2010.

Measures, C. I., Brown, M. T., Selph, K. E., Apprill, A., Zhou, M., Hatta, M., and Hiscock, W. T.: The influence of shelf processes in delivering dissolved iron to the HNLC waters of the Drake Passage, Antarctica, Deep-Sea Res. Pt. II, 90, 77–88, doi:10.1016/j.dsr2.2012.11.004, 2013.

Metzl, N., Brunet, C., Jabaud-Jan, A., Poisson, A., and Schauer, B.: Summer and winter air–sea CO_2 fluxes in the Southern Ocean, Deep-Sea Res., 53, 1548–1563, doi:10.1016/j.dsr.2006.07.006, 2006.

Moore, J. K., Doney, S. C., and Lindsay, K.: Upper ocean ecosystem dynamics and iron cycling in a global three-dimensional model, Global Biogeochem. Cy., 18, GB4028, doi:10.1029/2004GB002220, 2004.

Obernosterer, I., Christaki, U., Lefèvre, D., Catala, P., Van Wambeke, F., and Lebaron, P.: Rapid bacterial mineralization of organic carbon produced during a phytoplankton bloom induced by natural iron fertilization in the Southern Ocean, Deep-Sea Res. Pt. II, 55, 777–789, doi:10.1016/j.dsr2.2007.12.005, 2008.

O'Neill, L. P., Benitez-Nelson, C. R., Styles, R. M., Tappa, E., and Thunell, R. C.: Diagenetic effects on particulate phosphorus samples collected using formalin poisoned sediment traps, Limnol. Oceanogr.-Meth., 3, 308–317, doi:10.4319/lom.2005.3.308, 2005.

Park, Y.-H., Charriaud, E., Pino, D. R., and Jeandel, C.: Seasonal and interannual variability of the mixed layer properties and steric height at station KERFIX, southwest of Kerguelen, J. Marine Syst., 17, 571–586, doi:10.1016/S0924-7963(98)00065-7, 1998.

Park, Y.-H., Fuda, J.-L., Durand, I., and Naveira Garabato, A. C.: Internal tides and vertical mixing over the Kerguelen Plateau, Deep-Sea Res. Pt. II, 55, 582–593, doi:10.1016/j.dsr2.2007.12.027, 2008a.

Park, Y.-H., Roquet, F., Durand, I., and Fuda, J.-L.: Large-scale circulation over and around the Northern Kerguelen Plateau, Deep-Sea Res. Pt. II, 55, 566–581, doi:10.1016/j.dsr2.2007.12.030, 2008b.

Peterson, M. L., Wakeham, S. G., Lee, C., Askea, M. A., and Miquel, J. C.: Novel techniques for collection of sinking particles in the ocean and determining their settling rates, Limnol. Oceanogr.-Meth., 3, 520–532, doi:10.4319/lom.2005.3.520, 2005.

Picheral, M., Guidi, L., Stemmann, L., Karl, D. M., Iddaoud, G., and Gorsky, G.: The Underwater Vision Profiler 5: an advanced instrument for high spatial resolution studies of particle size spectra and zooplankton, Limnol. Oceanogr.-Meth., 8, 462–473, doi:10.4319/lom.2010.8.462, 2010.

Pinkerton, M. H., Smith, A. N. H., Raymond, B., Hosie, G. W., Sharp, B., Leathwick, J. R., and Bradford-Grieve, J. M.: Spatial and seasonal distribution of adult Oithona similis in the Southern Ocean: predictions using boosted regression trees, Deep-Sea Res., 57, 469–485, doi:10.1016/j.dsr.2009.12.010, 2010.

Planchon, F., Ballas, D., Cavagna, A.-J., van der Merwe, P., Bowie, A. W., Trull, T. W., Laurenceau, E., Davis, D. M., and Dehairs, F.: Carbon export in the naturally iron-fertilized Kerguelen area of the Southern Ocean using ^{234}Th-based approach, Biogeosciences, in preparation, 2014.

Pollard, R., Sanders, R., Lucas, M., and Statham, P.: The Crozet natural iron bloom and export experiment (CROZEX), Deep-Sea Res. Pt. II, 54, 1905–1914, doi:10.1016/j.dsr2.2007.07.023, 2007.

Pollard, R. T., Salter, I., Sanders, R. J., Lucas, M. I., Moore, C. M., Mills, R. A., Statham, P. J., Allen, J. T., Baker, A. R., Bakker, D. C. E., Charette, M. A., Fielding, S., Fones, G. R., French, M., Hickman, A. E., Holland, R. J., Hughes, J. A., Jickells, T. D., Lampitt, R. S., Morris, P. J., Nédélec, F. H., Nielsdóttir, M., Planquette, H., Popova, E. E., Poulton, A. J., Read, J. F., Seeyave, S., Smith, T., Stinchcombe, M., Taylor, S., Thomalla, S., Venables, H. J., Williamson, R., and Zubkov, M. V.: Southern Ocean deep-water carbon export enhanced by natural iron fertilization, Nature, 457, 577–580, doi:10.1038/nature07716, 2009.

Redfield, A.: On the Proportions of Organic Derivatives in Sea Water and their Relation to the Composition of Plankton, James Johnstone Meml. Vol. Univ. Press, Liverpool, 177–192, 1934.

Rembauville, M., Blain, S., Armand, L., Quéguiner, B., and Salter, I.: Export fluxes in a naturally fertilized area of the Southern Ocean, the Kerguelen plateau: ecological vectors of carbon and biogenic silica to depth (Part 2), Biogeosciences Discuss., 11, 17089–17150, doi:10.5194/bgd-11-17089-2014, 2014.

Rivkin, R. B. and Legendre, L.: Biogenic carbon cycling in the upper ocean: effects of microbial respiration, Science, 291, 2398–2400, doi:10.1126/science.291.5512.2398, 2001.

Rynearson, T. A., Richardson, K., Lampitt, R. S., Sieracki, M. E., Poulton, A. J., Lyngsgaard, M. M., and Perry, M. J.: Major contribution of diatom resting spores to vertical flux in the sub-polar North Atlantic, Deep-Sea Res., 82, 60–71, doi:10.1016/j.dsr.2013.07.013, 2013.

Salter, I., Lampitt, R. S., Sanders, R., Poulton, A., Kemp, A. E. S., Boorman, B., Saw, K., and Pearce, R.: Estimating carbon, silica and diatom export from a naturally fertilised phytoplankton bloom in the Southern Ocean using PELAGRA: a novel drifting sediment trap, the crozet natural iron bloom and export experiment CROZEX, Deep-Sea Res. Pt. II, 54, 2233–2259, doi:10.1016/j.dsr2.2007.06.008, 2007.

Salter, I., Kemp, A. E. S., Lampitt, R. S., and Gledhill, M.: The association between biogenic and inorganic minerals and the amino acid composition of settling particles, Limnol. Oceanogr., 55, 2207–2218, doi:10.4319/lo.2010.55.5.2207, 2010.

Salter, I., Kemp, A. E. S., Moore, C. M., Lampitt, R. S., Wolff, G. A., and Holtvoeth, J.: Diatom resting spore ecology drives enhanced carbon export from a naturally iron-fertilized bloom in the Southern Ocean: eucampia driven carbon fluxes, Global Biogeochem. Cy., 26, GB1014, doi:10.1029/2010GB003977, 2012.

Salter, I., Schiebel, R., Ziveri, P., Movellan, A., Lampitt, R., Wolff, G. A. Carbonate counter pump stimulated by natural iron fertilization in the Polar Frontal Zone, Nat. Geosci. , 7, 885–889, 2014.

Sarmiento, J. L. and Gruber, N.: Ocean Biogeochemical Dynamics, Princeton University Press, Princeton, 2006.

Sarmiento, J. L. and Le Quéré, C.: Oceanic carbon dioxide uptake in a model of century-scale global warming, Science, 274, 1346–1350., 1996.

Savoye, N., Benitez-Nelson, C., Burd, A. B., Cochran, J. K., Charette, M., Buesseler, K. O., Jackson, G. A., Roy-Barman, M., Schmidt, S., and Elskens, M.: ^{234}Th sorption and export models in the water column: a review, future applications of ^{234}Th in aquatic ecosystems (FATE), Mar. Chem., 100, 234–249, doi:10.1016/j.marchem.2005.10.014, 2006.

Savoye, N., Trull, T. W., Jacquet, S. H. M., Navez, J., and Dehairs, F.: ^{234}Th-based export fluxes during a natural iron fertilization experiment in the Southern Ocean (KEOPS), KEOPS: Kerguelen ocean and plateau compared study, Deep-Sea Res. Pt. II, 55, 841–855, doi:10.1016/j.dsr2.2007.12.036, 2008.

Schlitzer, R.: Export production in the Equatorial and North Pacific derived from dissolved oxygen, nutrient and carbon data, J. Oceanogr., 60, 53–62, 2004.

Schulz, M. and Mudelsee, M.: REDFIT: estimating red-noise spectra directly from unevenly spaced paleoclimatic time series, Comput. Geosci., 28, 421–426, doi:10.1016/S0098-3004(01)00044-9, 2002.

Seeyave, S., Lucas, M. I., Moore, C. M., and Poulton, A. J.: Phytoplankton productivity and community structure in the vicinity of the Crozet Plateau during austral summer 2004/05, the crozet natural iron bloom and export experiment CROZEX, Deep-Sea Res. Pt. II, 54, 2020–2044, doi:10.1016/j.dsr2.2007.06.010, 2007.

Smetacek, V., Assmy, P., and Henjes, J.: The role of grazing in structuring Southern Ocean pelagic ecosystems and biogeochemical cycles, Antarct. Sci., 16, 541–558, doi:10.1017/S0954102004002317, 2004.

Tarling, G. A., Ward, P., Atkinson, A., Collins, M. A., and Murphy, E. J.: DISCOVERY 2010: spatial and temporal variability in a dynamic polar ecosystem, Deep-Sea Res. Pt. II, 59–60, 1–13, doi:10.1016/j.dsr2.2011.10.001, 2012.

Thomalla, S. J., Fauchereau, N., Swart, S., and Monteiro, P. M. S.: Regional scale characteristics of the seasonal cycle of chlorophyll in the Southern Ocean, Biogeosciences, 8, 2849–2866, doi:10.5194/bg-8-2849-2011, 2011.

Trull, T. W., Bray, S. G., Buesseler, K. O., Lamborg, C. H., Manganini, S., Moy, C., and Valdes, J.: In situ measurement of mesopelagic particle sinking rates and the control of carbon transfer to the ocean interior during the Vertical Flux in the Global Ocean (VERTIGO) voyages in the North Pacific, understanding the ocean's biological pump: results from VERTIGO, Deep-Sea Res. Pt. II, 55, 1684–1695, doi:10.1016/j.dsr2.2008.04.021, 2008a.

Trull, T. W., Davies, D., and Casciotti, K.: Insights into nutrient assimilation and export in naturally iron-fertilized waters of the Southern Ocean from nitrogen, carbon and oxygen isotopes, KEOPS: Kerguelen ocean and plateau compared study, Deep-Sea Res. Pt. II, 55, 820–840, doi:10.1016/j.dsr2.2007.12.035, 2008b.

Turner, J. T.: Zooplankton fecal pellets, marine snow and sinking phytoplankton blooms, Aquat. Microb. Ecol., 27, 57–102, doi:10.3354/ame027057, 2002.

Volk, T. and Hoffert, M. I.: Ocean carbon pumps: Analysis of relative strengths and efficiencies in ocean-driven atmospheric CO_2 changes, in: Geophysical Monograph Series, edited by: Sundquist, E. T. and Broecker, W. S., American Geophysical Union, Washington, DC, 99–110, 1985.

Table 1. Dynamics of carbon and nitrogen export fluxes at station A3 collected by the sediment trap at 289 m.

			Fluxes (mmol m^{-2} d^{-1})			Contribution to annual export (%)	
Cup	Start	Stop	POC	PON	POC : PON	POC	PON
1	21 Oct 2011	04 Nov 2011	0.15 ± 0.01	0.02 ± 0.00	6.80 ± 0.56	2.11 ± 0.06	2.30 ± 0.01
2	04 Nov 2011	18 Nov 2011	0.14 ± 0.01	0.02 ± 0.00	6.09 ± 0.67	1.94 ± 0.16	2.27 ± 0.15
3	18 Nov 2011	02 Dec 2011	0.15 ± 0.01	0.02 ± 0.00	7.33 ± 0.31	2.12 ± 0.06	1.99 ± 0.06
4	02 Dec 2011	12 Dec 2011	1.60 ± 0.04	0.23 ± 0.01	6.95 ± 0.29	16.18 ± 0.45	16.48 ± 0.07
5	12 Dec 2011	22 Dec 2011	0.34 ± 0.00	0.05 ± 0.00	6.87 ± 0.08	3.41 ± 0.03	3.64 ± 0.03
6	22 Dec 2011	01 Jan 2012	0.51 ± 0.04	0.08 ± 0.01	6.70 ± 0.78	4.82 ± 0.76	5.50 ± 0.39
7	01 Jan 2012	11 Jan 2012	0.42 ± 0.02	0.06 ± 0.00	6.73 ± 0.46	4.23 ± 0.14	4.65 ± 0.42
8	11 Jan 2012	25 Jan 2012	0.34 ± 0.01	0.05 ± 0.00	6.94 ± 0.38	4.83 ± 0.18	4.84 ± 0.11
9	25 Jan 2012	08 Feb 2012	1.47 ± 0.03	0.20 ± 0.01	7.38 ± 0.26	20.98 ± 0.57	21.07 ± 0.05
10	08 Feb 2012	22 Feb 2012	0.55 ± 0.04	0.08 ± 0.00	6.97 ± 0.88	7.83 ± 0.64	8.36 ± 0.57
11	22 Feb 2012	31 May 2012	0.27 ± 0.01	0.03 ± 0.00	8.09 ± 0.22	26.84 ± 0.47	24.12 ± 0.20
12	31 May 2012	07 Sep 2012	0.04 ± 0.00	0.01 ± 0.00	6.06 ± 0.17	4.71 ± 0.90	4.78 ± 0.09
Annual export (mmol m^{-2} yr^{-1})			98.24 ± 4.35	13.59 ± 0.30			

Title Page
Abstract | Introduction
Conclusions | References
Tables | Figures
◀| |▶
◀ ▶
Back | Close
Full Screen / Esc
Printer-friendly Version
Interactive Discussion

Table 2. Number of swimmer individuals found in each cup and swimmer intrusion rate (number d^{-1}, bold numbers) for each taxa and for the total swimmers.

Cup	Copepod	Pteropod	Euphausid	Ostracod	Amphipod	Cnidarian	Polychaete	Ctenophore	Siphonophore	Salp	Total
1	166	13	1	2	1	0	0	0	0	0	183
	12	**1**	**<1**	**<1**	**<1**	**0**	**0**	**0**	**0**	**0**	**13**
2	55	0	0	0	0	0	0	0	0	0	55
	4	**0**	**0**	**0**	**0**	**0**	**0**	**0**	**0**	**0**	**4**
3	0	0	0	0	0	0	0	0	0	0	0
	0	**0**	**0**	**0**	**0**	**0**	**0**	**0**	**0**	**0**	**0**
4	113	0	0	0	0	0	0	0	0	0	113
	11	**0**	**0**	**0**	**0**	**0**	**0**	**0**	**0**	**0**	**11**
5	0	0	0	0	0	0	0	0	0	0	0
	0	**0**	**0**	**0**	**0**	**0**	**0**	**0**	**0**	**0**	**0**
6	540	0	1	0	2	5	1	4	1	0	554
	54	**0**	**<1**	**0**	**<1**	**<1**	**0**	**0**	**0**	**0**	**55**
7	583	0	0	0	0	2	2	3	0	0	590
	58	**0**	**0**	**0**	**0**	**<1**	**<1**	**<1**	**0**	**0**	**58**
8	686	33	2	2	8	5	1	4	0	0	741
	49	**2**	**<1**	**<1**	**1**	**<1**	**<1**	**<1**	**0**	**0**	**52**
9	392	14	4	3	121	4	2	0	0	0	540
	28	**1**	**<1**	**<1**	**9**	**<1**	**<1**	**0**	**0**	**0**	**38**
10	264	69	1	2	18	11	0	2	0	0	367
	19	**5**	**<1**	**<1**	**1**	**1**	**0**	**<1**	**0**	**0**	**26**
11	54	0	0	0	29	4	1	0	0	0	88
	1	**0**	**0**	**0**	**<1**	**<1**	**<1**	**0**	**0**	**0**	**1**
12	1481	44	5	7	2	3	2	0	0	1	1544
	15	**<1**	**<1**	**<1**	**<1**	**<1**	**<1**	**0**	**0**	**<1**	**15**

Table 3. Synthesis of estimates of POC fluxes at the base of, or under, the mixed layer at station A3 from the KEOPS 1 cruise.

Author	Method	Period	Depth (m)	POC flux (mmol m^{-2} d^{-1})
Savoye et al. (2008)	^{234}Th deficit and local C conversion factor	23 Jan–12 Feb 2005	100	23 ± 3.6
			150	25.7 ± 3.6
			200	24.5 ± 6.8
Ebersbach and Trull (2008)	Drifting gel trap, optical measurements and constant C conversion factor	4 Feb 2005	200	24
			220	5.2
		12 Feb 2005	330	0.7
			430	1
Jouandet et al. (2008)	Annual DIC budget	Annual	MLD basis	85
Trull et al. (2008b)	Drifting sediment trap	4 Feb 2005	200	7.3–10
		12 Feb 2005		3–3.1
Jouandet et al. (2011)	In situ optical measurement (UVP) and power function C conversion factor	22 Jan 2005	220	72.4
			330	27.2
			400	21.6
		23 Jan 2005	220	29.8
			330	26.8
			400	15.9
		12 Feb 2005	220	4.8
			330	5.6
			400	7.9

Title Page
Abstract Introduction
Conclusions References
Tables Figures
◀| |▶
◀ ▶
Back Close
Full Screen / Esc
Printer-friendly Version
Interactive Discussion

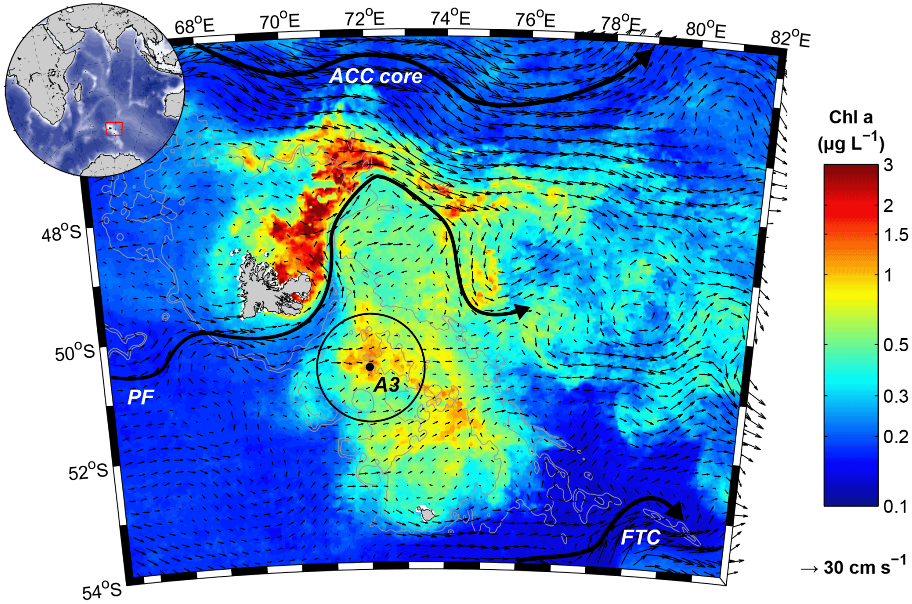

Figure 1. Localization of the Kerguelen Plateau in the Indian sector of the Southern Ocean and detailed map of the satellite-derived surface chlorophyll *a* concentration (MODIS level 3 product) averaged over the sediment trap deployment period. Sediment trap location at the A3 station is represented by a black dot, whereas the black circle represents the 100 km radius area used to average the surface chlorophyll *a* time series. Arrows represent surface geostrophic circulation derived from the absolute dynamic topography (AVISO product). Positions of the Antarctic Circumpolar Current core (AAC core), the Polar Front (PF) and the Fawn Through Current (FTC) are shown by thick black arrows. Grey lines are 500 and 1000 m isobaths.

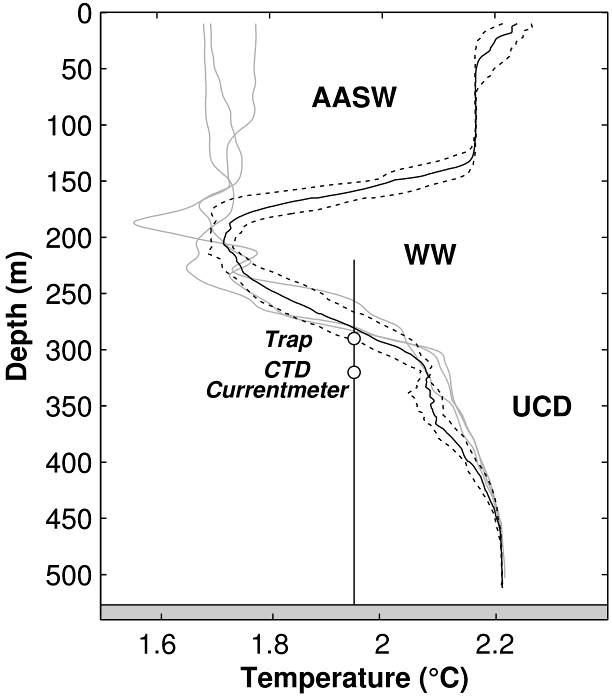

Figure 2. Schematic of the instrumented mooring line against vertical temperature profiles. The sediment trap and the current meter/CTD sensor location on the mooring line are shown by white circles. Temperature profiles performed during the sediment trap deployment (20 October 2011) are represented by grey lines. Black full line is the median temperature profile from 12 casts realized on the 16 November 2011. Dashed black lines are the first and third quartiles from these casts. The grey rectangle represents the Kerguelen Plateau seafloor. The different water masses are Antarctic Surface Water (AASW), Winter Water (WW) and Upper Circumpolar Deep Water (UCDW).

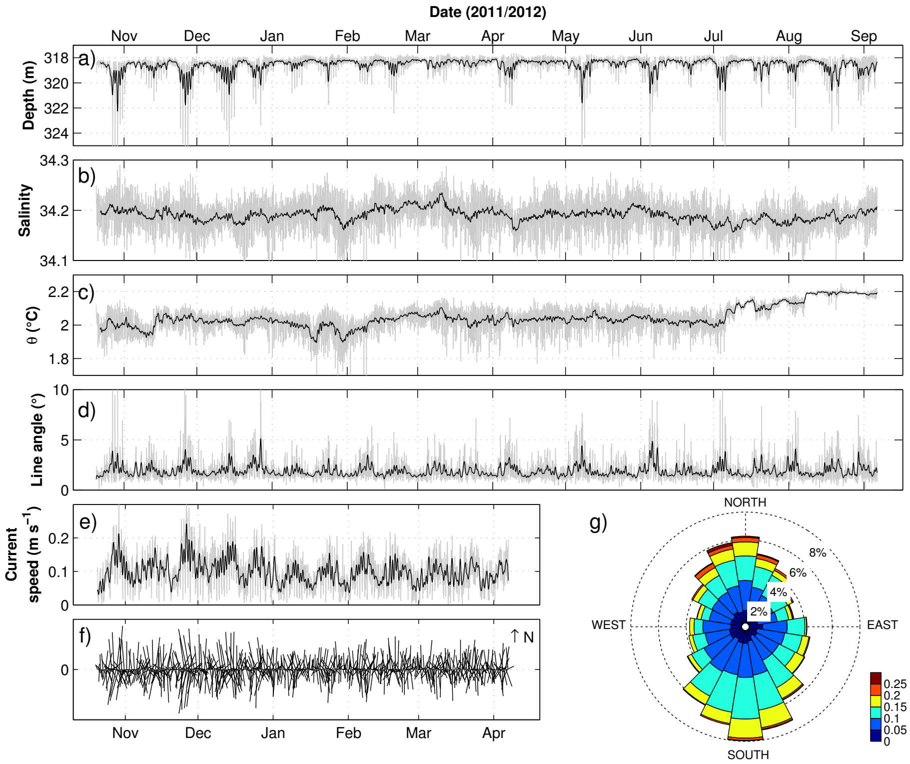

Figure 3. Hydrological properties recorded by the instrument mooring at station A3. **(a)** Depth of the CTD sensor, **(b)** salinity, **(c)** potential temperature, **(d)** line angle, **(e)** current speed, grey lines are raw data, black lines are low-pass filtered data with a Gaussian filter (40 h window as suggested by the spectral analysis), **(f)** direction and speed of currents represented by vectors (under sampled with a 5 h interval) and **(g)** wind rose plot of current direction and intensities, dotted circles are directions relatives frequencies and colors refer to current speed ($\mathrm{m\,s^{-1}}$).

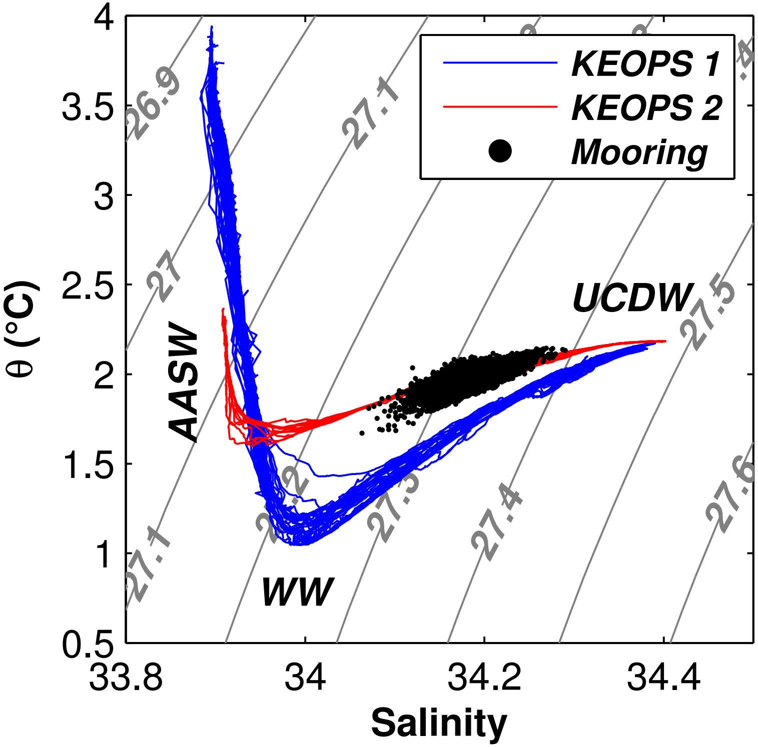

Figure 4. Potential temperature/salinity diagram at station A3. Data are from the moored CTD (black dots), KEOPS1 (blue line) and KEOPS2 (red line). Grey lines are potential density anomaly. The different water masses are Antarctic Surface Water (AASW), Winter Water (WW) and Upper Circumpolar Deep Water (UCDW).

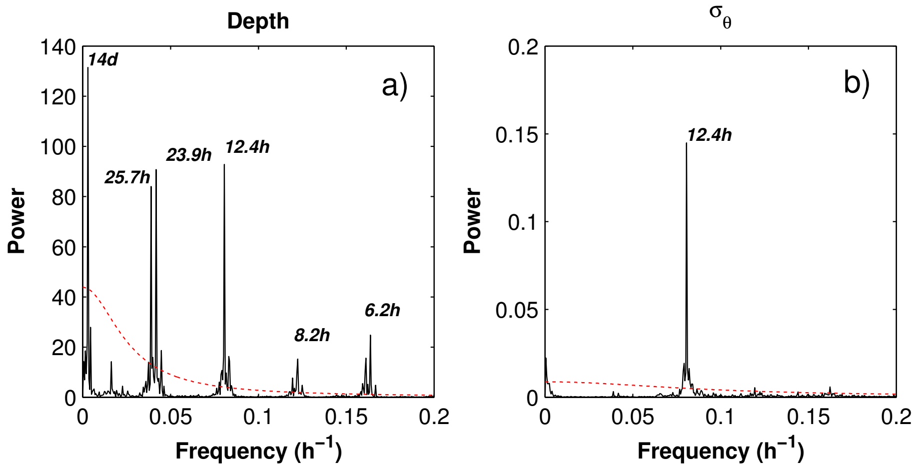

Figure 5. Power spectrum of the spectral analysis of **(a)** depth time series and **(b)** potential density anomaly time series. Pure red noise (null hypothesis) is represented by red dashed lines for each variable. The period corresponding to a significant power peak (power peak higher than the red noise) is written.

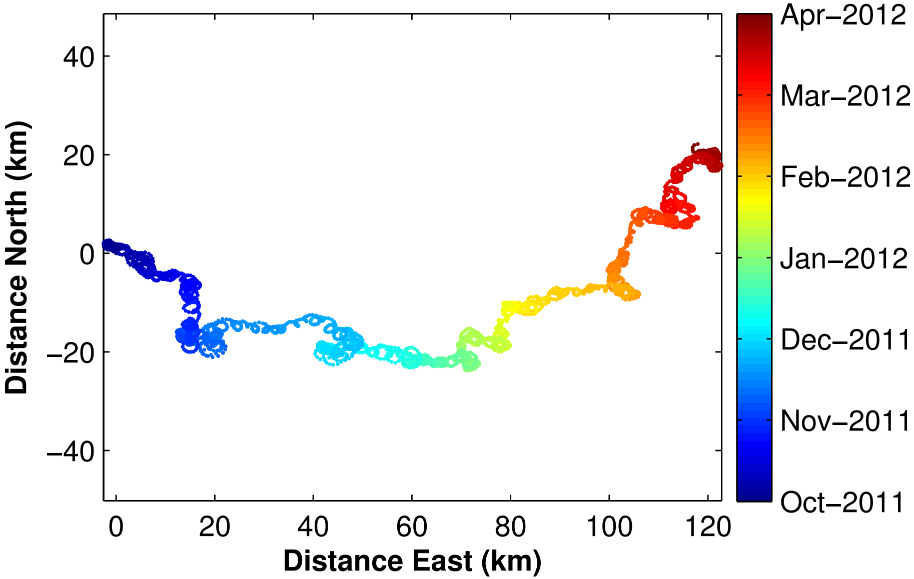

Figure 6. Progressive vector diagram calculated from current meter data at 319 m. The color scale refers to date.

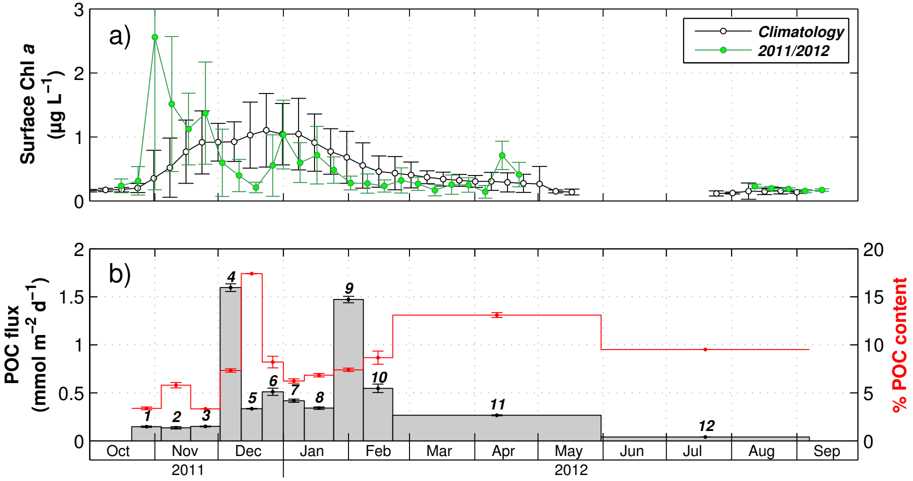

Figure 7. Seasonal variations of surface chlorophyll *a* and particulate organic carbon (POC) export. **(a)** Seasonal surface chlorophyll concentration and 16 years climatology (Globcolour) averaged in a 100 km radius around the station A3 station. Error bars represent the inter annual standard deviation for the climatology, and the spatial standard deviation for the 2011/12 data. **(b)** POC flux (grey bars) and mass percentage of POC (red dotted line). Error bars are standard deviations from triplicates, bold italic numbers refer to cup number.

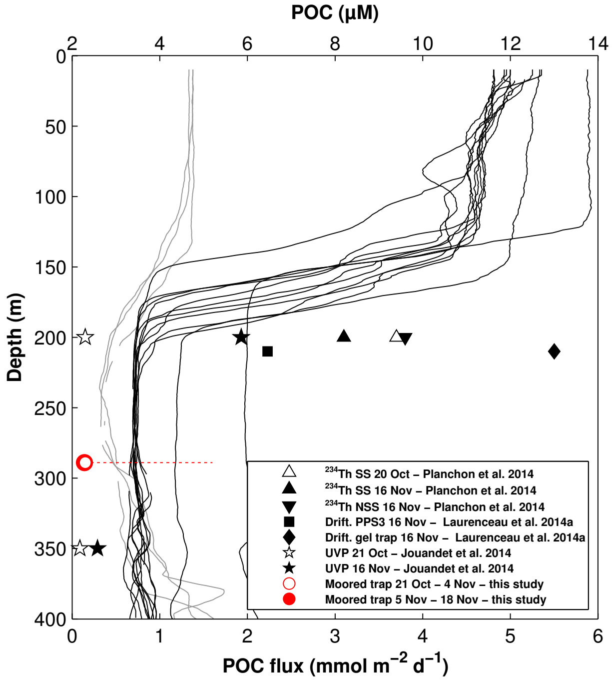

Figure 8. POC flux and stock at station A3 during the KEOPS2 cruise. Grey and dark lines represent vertical profiles of POC concentration derived from calibrated transmissiometer for 20 October and 16 November 2011, respectively. Triangles, circles, squares, diamonds and stars denote POC fluxes estimated by different approaches as referenced in the legend. Empty symbols represents the first visit (21 October 2011) and full symbols the second visit (16 November 2011). The red dotted line denotes the POC flux range observed in the sediment trap (0.05 to 1.6 mmol m^{-2} d^{-1}).

Title Page
Abstract
Introduction
Conclusions
References
Tables
Figures
◀▌ ▶▌
◀ ▶
Back
Close
Full Screen / Esc
Printer-friendly Version
Interactive Discussion